Coordinated Tap Changer Control

Theory and Practice

Mats Larsson

Lund 1997

The figure on the cover illustrates the conditions for existence of limit cycles due to interaction between an OLTC's dead-band and the load dynamics. The figure is explained in Section 6.5.

Abstract

This thesis deals with oscillation phenomena related to the discrete nature of tap changers. Two fundamentally different phenomena are investigated:

- oscillations due to interaction among the local control systems of cascaded tap changers
- self-sustained oscillations due to interaction between the tap changer control system dead-band and load dynamics

The first phenomenon is of importance for the normal state control, in that it leads to unnecessary operations of the tap changers and consequently unnecessary wear on the tap changer mechanism and poor voltage quality. Three means of reducing the interactions are proposed:

- new tuning for the existing (local) controllers
- a centralised optimal controller
- a centralised fuzzy rule-based controller

Results from simulations on the basis of load patterns recorded during different seasons in a rural distribution system indicate that the new tuning reduces daily the number of tap operations by some 10 % compared to the old tuning. The simulations indicate that the optimal and fuzzy-rule based controllers yield additional reductions of about 36 % and 45 % repectively, compared to the existing controllers with the new tuning. The simulations have been validated in a series of field tests using a prototype of the fuzzy rule-based controller.

The second phenomenon is of importance for the analysis of oscillatory voltage collapse. Using a small example system, it is shown that the results from analysis based on a continuous state OLTC model are unreliable, since the same system with a detailed OLTC model exhibits a limit cycle related

to the control system dead-band that will arrest the oscillatory voltage instability predicted by small disturbance analysis. The key parameters for the occurrence of limit cycles are identified as the system load level, degree of reactive compensation and the load voltage dependency. Adjusting OLTC control system parameters such as time delays or dead-band size are shown to have no effect on the existence of these limit cycles in certain loading conditions.

Acknowledgements

This thesis covers the work I have carried out at the Department of Industrial Electrical Engineering and Automation as part of a project on distribution automation (AED). I would like to thank my colleagues, especially the other two PhD candidates in the AED project: Johanna Persson (now with Ericsson Software Technology) and Olof Samuelsson, at the department for providing the atmosphere that makes it so much fun to go to work. Of course, special thanks go to my supervisors Gustaf Olsson and Daniel Karlsson at Sydkraft AB who suggested the topic of the thesis and made the preliminary investigations at Österlen, for their support and help. The members of the steering committee, Bo Eliasson, Lars Gertmar, Jan Rønne-Hansen, Gustaf Olsson and Thomas Pehrsson have provided valuable suggestions and guidance throughout the project. Jan Rønne-Hansen and Thomas Pehrsson also gave private lectures to introduce us (the three AED PhD candidates) to the field of power systems. David J. Hill of the University of Sydney have provided a lot of valuable input in our discussions during the project. Many thanks.

The field tests were carried out in a Sydkraft distribution system at Österlen in southern Sweden. The local personnel at Österlen and the personnel at the Sydkraft system operation center in Malmö were always very helpful (and indulgent towards the occasional mishap during the tests), especially Lennart Elgemark and Alf Larsen who were my contacts. Thanks also to the guys at IDA-lab who helped me get started with the LonWorks system and let me use their development facilities and Magnus Sommansson who handled the Sydkraft bureaucracy for me.

During February and March 1996, I had the pleasure of visiting the Systems and Control group at the University of Sydney, Australia. I would like to thank David J. Hill and Dragana H. Popović for the productive and inspiring time I spent there. They have both contributed significantly to the work presented in Chapter 6. Also, the help in getting installed there provided by Stefan Johansson and Colleen Moore and the cricket lessons by my friends

at Susan Street were much appreciated.

The work has been financially supported by Elforsk and Sydkraft AB, this support is gratefully acknowledged.

Last, but certainly not least, I would like to thank my friends and family for their support over the years.

Lund, May 11, 1997,

Mats Larsson

Contents

1

Introduction

Today's scientific question is: What in the world is electricity and where does it go after it leaves the toaster?

Dave Barry, "What is Electricity?"

1.1 Problems and Possibilities

The purpose of voltage control in distribution networks is to compensate for load variations and events in the transmission system, such that all customer supply voltages are kept within certain bounds. A number of on-load tap changers *(OLTCs)*, each capable of regulating the voltage of the secondary side of a transformer at one point in the network, are available in the distribution systems for this purpose. The control is discrete-valued, typically with steps of 1-3 %. Figure 1.1 shows the structure of a typical Swedish distribution network. The systems are typically radial, with tap changers cascaded in up to three levels. Therefore, interaction among OLTCs at different voltage levels is possible. OLTC control is presently based on a local voltage measurement in each sub-station, with no coordination of OLTCs on different voltage levels or in different branches of the network.

Figure 1.2 shows a voltage measurement recorded in a preliminary study [Karlsson, 1993] at a 10 kV sub-station with the conventional voltage control in operation. The sub-station is supplied through three cascaded tap changing transformers. There were 24 *voltage steps* during the 150 minute recording. Nine of the steps are due to tap operations in the sub-station in question (marked ± 1), and the rest are due to tap operations and capacitor bank switchings higher up in the network. Most of the tap operations

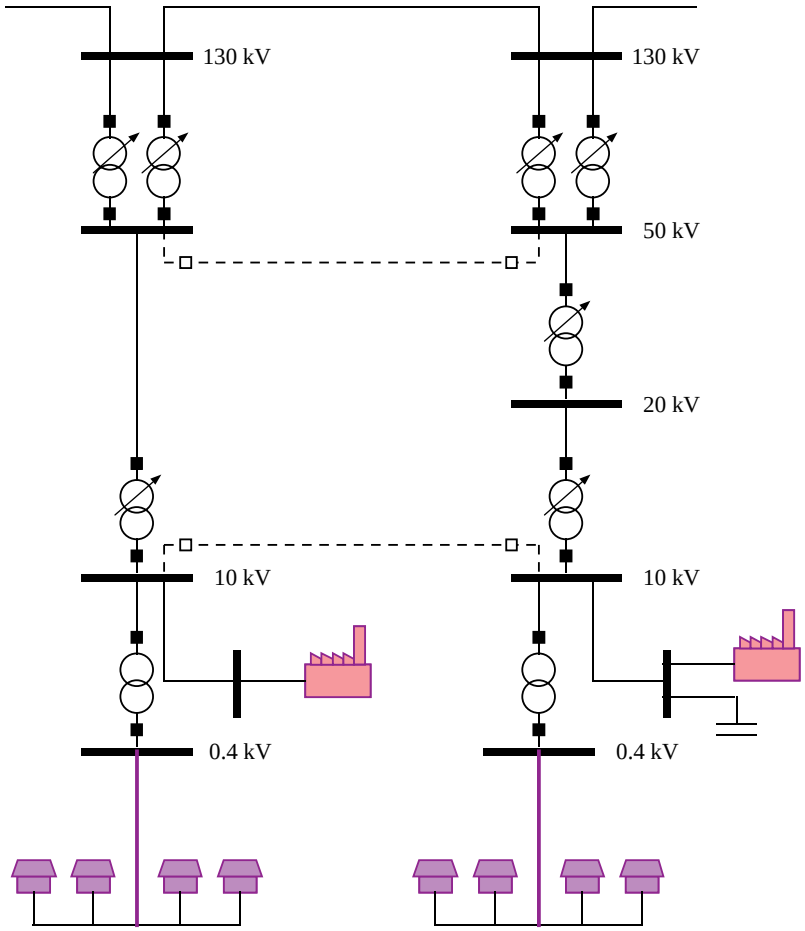

Figure 1.1 Typical structure of a Swedish distribution system. Transformers with OLTCs are marked with an arrow.

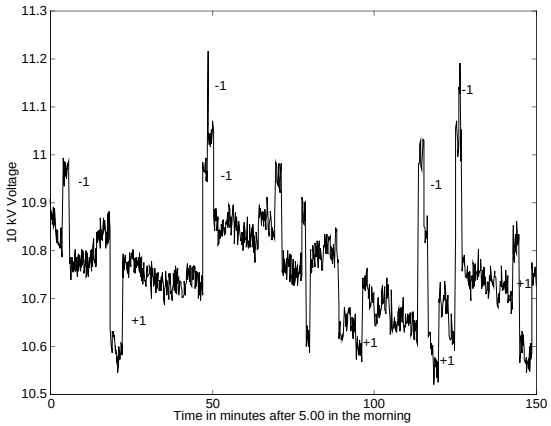

Figure 1.2 Field measurement of the voltage in the 10 kV sub-station at Östra Tommarp during load pickup. The tap operations made at ÖTP are marked with +/-1.

made in the sub-station counteract the effect of tap changers higher up in the network.

Poor coordination of cascaded tap changers can be dangerous from a voltage stability point of view. A sudden voltage drop in the feeding network may result in considerable voltage overshoot at the load level [Karlsson, 1992, Altsjö, 1993] (compare Figure 3.2). Since loads are voltage sensitive, this will increase the loading of the feeding transmission system. Disturbances of this type are likely to arise during voltage instability incidents as a result of tripped lines or generation units in the transmission system. During such incidents, the transmission system is already operating close to its transfer limits and increased loading is highly undesirable.

With coordinated control of tap changers, it should be possible to reduce the number of, or eliminate counteracting tap operations. Consequently, the total number of operations and the number of voltage spikes due to OLTC interaction would decrease. Wear on the tap changer mechanism is the most common reason for transformer maintenance, and therefore a reduction of the number of tap operations made is highly desirable. Referring to the role of OLTCs in voltage instability incidents, the new control schemes presented in this thesis can prevent voltage overshoot due to voltage drops in the feeding system. With coordinated control, it would also be possible to use alternative control strategies during voltage instability incidents.

1.2 Outline and Contributions

The thesis mainly deals with coordination of the normal state control of OLTCs and is a result of the project on Distribution Automation that has been going on at the Department since July 1993. The thesis demonstrates coordinated OLTC control as one application of distribution automation.

The natural starting point of the work on coordinated OLTC control was to investigate to what extent the problem of OLTC interaction could be solved by re-tuning the existing controllers. This investigation resulted in a tuning recommendation which gradually assigns larger time delay for lower level OLTCs, thereby reducing OLTC interaction for large step disturbances. Such disturbances occur on a daily basis, for example when capacitor banks are switched in the feeding network. However, the problem persists with regard to the disturbances introduced by the daily load variations.

The next step was to investigate to what degree communication between sub-stations can further improve the control. First, an optimal controller based on on-line tap optimisation was developed. This controller eliminates OLTC interaction, but relies on a perfect network model and measurements of the load powers. This was not considered acceptable for the actual implementation, and therefore a simpler rule-based control scheme was developed. This control scheme offers near-optimal performance without the drawbacks of the optimal controller.

An important aim was also to demonstrate the feasibility of coordinated voltage control as an application of DA. A prototype was designed and installed in the distribution system at Österlen in southern Sweden. Using the prototype, a number of load patterns were recorded. On the basis of these load patterns the control schemes were compared by simulation. The prototype was also used to validate these simulation results.

The other topic of the thesis is OLTC modelling under high load conditions. This investigation was motivated by the lack of a well-established practice for OLTC modelling in voltage stability studies. During this study, it was shown that OLTC control system dead-bands may interact with load dynamics, thereby creating a limit cycle phenomenon that can arrest oscillatory voltage instability predicted by small-disturbance analysis based on an OLTC model neglecting the dead-band. The thesis is organised in the following sections:

Introduction (Chapter 1)

- an introduction to distribution automation

Problem Formulation (Chapter 2)

- description of the disturbances that affect the voltage control
- modelling of the relevant power system components
- description of a three OLTC test network at Österlen

Controller Synthesis (Chapter 3)

- derivation of a tuning recommendation for the existing local controllers that yield selectivity for step disturbances
- derivation of a new control scheme based on on-line tap optimisation and communication that yield selectivity for general disturbances
- derivation of a new control scheme based on fuzzy set manipulation and communication that yield selectivity for general disturbances

Prototype (Chapter 4)

- description of the prototype controller and the installation in the Österlen test system

Evaluation and Validation in a Field Test (Chapter 5)

- simulation results on the basis of load patterns recorded in the Österlen test system
- validation of the simulations using the prototype controller
- simulation results for a full distribution system

Dynamic Modelling of OLTCs (Chapter 6)

- presentation of a previously unknown limit cycle phenomena due to OLTC dead-bands and load-tap interaction that in certain load conditions arrests oscillatory voltage instability

Terms written in *italics* at the place of their first reference, have a special meaning in the text that may or may not be the same as (what the reader thinks is) the prevalent meaning. Uncertain readers are advised to look those up in the glossary in Appendix B. In this appendix, there is also a nomenclature explaining the various symbols used in the text.

1.3 Publications

Larsson, M. and Karlsson, D. (1995), Coordinated control of cascaded tap changers in a Radial distribution network. In *Proceedings of IEEE-KTH Stockholm PowerTech Conference, June 18-22.* Publication SPT PS 22-06-0405.

Larsson, M. (1996), Coordinated control of cascaded tap changers in a radial distribution network, *Preprints from Reglermötet, Högskolan i Luleå, June 6-7.*

Larsson, M., Popović D. and Hill, D.J. (1997), Limit cycles in power systems due to OLTC dead-bands and load-voltage dynamics, Submitted for publication in *Journal of Electric Power Systems Research.*

1.4 Structure of the Swedish Power System

The primary function of an electric power system is to meet the customer demand of electric power. The system has to do so while being subject to a number of constraints, for example that the supply voltages and the loading of each system component is in accordance with the operational limits. Apart from these constraints, there is a secondary objective to minimise operational cost, for example by minimising losses or rescheduling output of generators. The power system must be robust to the faults that sometimes arise in the system, so that unnecessary blackouts are avoided. These objectives and constraints form, taken together, an extremely complex problem which must be decomposed to be solved. Traditionally, electric power systems are divided into three main parts: the generation system responsible for economic production of the present demand; the transmission system responsible for transporting energy from the main generation to the main load areas; and the distribution system responsible for transporting energy within the load areas, to the customers. This division pervades the power industry organisation as a whole. Often different companies or at least different divisions are responsible for each of the three systems.

Hydroelectric and nuclear power are the two dominating sources of generation in Sweden, each yielding almost 50 % of the total power demand. Oil and gas power plants are in use during peak load conditions. The transmission system is extensively meshed and has voltage levels of 400 and 220 kV *(VHV)*. Since hydro production is concentrated in the North and load is concentrated in the South of Sweden, the bulk transmission system is longitudinal, stretching more than 1500 kilometres from North to South. A number of 130 kV *(HV)* buses are used in the slightly meshed sub-transmission network. 50 kV, 20 kV, 10 kV *(MV)* and 0.4 kV *(LV)* busbars are present in the distribution system. Figure 1.1 shows a schematic of a typical distribution system. Under normal circumstances, the meshes are broken by the opening of the circuit breakers on the tie lines at the MV and LV levels. Therefore, the distribution system is radial under normal configuration. This is a common configuration of Swedish distribution networks. Up to three levels of cascaded OLTCs regulate customer side voltages in rural areas where the distribution systems tend to be weak, whereas in one or two levels are considered to be sufficient in stronger networks. Shunt capacitors and reactors are common in the transmission system. In addition, some MV customers have their own reactive power compensation. Most often, there is no automatic voltage control at the 10/0.4 kV transformers.

In the early development, automation was considered expensive by the power industry, and the robustness problem has to a large extent been solved by installing excess capacity rather than automation, especially in distribution systems. Following the development in computer and communication technology during the last decades, extensive automation in the transmission networks (*SCADA*) has been installed. Examples of this are: control of transmission network actuators for loss minimisation (*Optimal Power Flow, OPF*) and optimal scheduling of generation output for economic operation (*Unit Commitment, UC*). The early academic results on these applications appeared in the sixties and early seventies. These systems are now widely used in the generation and transmission industry.

1.5 Distribution Automation

Distribution automation *(DA)* is foreseen to automate the distribution systems in the same way the SCADA systems have done in the transmission and generation systems. The term distribution SCADA is sometimes used synonymously with distribution automation. Some applications of DA that have been suggested are:

Coordinated Voltage/Reactive Power Control
Control of reactive power transport reduces losses and thereby cost of operation. Coordination improves control in terms of fewer control actions as well as improved voltage profile. Centralised voltage control also introduces the possibility of using alternative control strategies for stressed operating conditions. It also reduces maintenance and operational costs, and improves system security. [Larsson and Karlsson, 1995, Roytelman et al., 1995]

Direct Load Control
Utility controlled load management, for example automatic load shedding for use in emergencies or scheduling of controllable loads to reduce daily load variations. It improves system security and reduces impact of emergency load shedding.

Automatic Feeder Reconfiguration
Today, distribution feeders are reconfigured twice a year in Sydkraft's network's, at best, to cope with the seasonal load variations. Optimal distribution network configuration in terms of losses and security can be found automatically on a weekly or even daily basis. With coordinated voltage control and protection systems distribution systems do not need to be operated radially. This reduces operational cost. [Nara et al., 1992]

Fault Detection/Location and Automatic Sectionalising
Automatic detection and localisation of faults help the repair personnel locate the fault for quick repair. Sectionalising after a fault can be done automatically, quickly isolating the fault. The automatic feeder reconfiguration system can then be used to find a new, temporary, network configuration for use while the system is under repair. Since faults can be detected and located more rapidly, it reduces outage time and thereby customer inconvenience and lost sales. [Partanen et al., 1994]

Customer Relations
This includes for example on-line voltage quality measurement and remote meter reading. Indirect load control, using dynamic pricing as an incentive offers new services to customers and may also improve system security.

We see that a number of benefits from DA can be expected, in terms of security, transfer capability, voltage quality and reduced maintenance costs. However, all the DA applications discussed here rely on improved distribution system state knowledge and controllability. Communication facilities are essential since most functions rely on centralised or coordinated control at some level. Some functions, for example indirect load control, require communication all the way down to the customer level and are therefore the most costly to implement, whereas some other functions like coordinated voltage control or feeder reallocation schemes can be effectively used on the MV level. The fact that it is possible to use the same communication infrastructure for the different functions should be exploited and it is the author's opinion that it has to be done in order to make DA cost-effective. This makes standardisation issues an important aspect of DA. The IEC, CIGRE, EdF, IEEE and EPRI all have their own working groups looking into this matter [Lee-Smith, 1996]. Although the majority of work in this field has been company or application specific, Lee-Smith foresees that a standard is accepted by the American power industries within the next two years.

1.6 Home Automation

Another branch of automation, which is relevant to DA, is Home Automation *(HA)*. The introduction of HA aims at improving living comfort, security and/or reducing running costs of a household by means of automation. Some specific functions are lighting control, security- and energy management. X10, CEBus and LonWorks are three of the most widely used communication standards. The energy management functions of HA are very closely related to DA, for example indirect load control using dynamic pricing assumes that there is intelligent control at the customer side. In these applications, HA will interact with DA. A typical HA energy management function is coordinated control of water heaters and electric space heating such that they are not operating simultaneously to minimise the maximum power demand of the household. Using dynamic pricing, a DA indirect load control system may persuade the HA system to switch out both heating systems during peak load conditions. Similar energy management functions are being discussed within various energy-intensive industries. In this way the interaction among HA and DA systems offers benefits to customers as well as utilities. One example of dynamic load control has been examined by [Ericsson, 1997].

2

The Control Problem

When the speaker and he to whom he is speaks do not understand, that is metaphysics.

Voltaire

2.1 The Physics in a Distribution Network

The basic physical phenomena that create the need for voltage control can be understood from Figure 2.1. It illustrates the couplings between the different physical quantities involved. In the following sections, these are illustrated by simulation of the simple radial distribution system in Figure 2.2. The system is a model of the system feeding the Tomelilla (TLA) distribution system down to the 50 kV bus-bar. An ideal generator feeds a distribution system through a transmission system equivalent ($Z_0 \angle \theta_0$). The distribution system is modelled as an ideal transformer in series with a distribution system impedance. The distribution load has been aggregated at bus 2. Relevant system parameter values are given in Appendix A.1.

Line Voltage Drop

Consider a power transport through the impedance ($Z_0 \angle \theta_0$) in Figure 2.2. The active and reactive power received at bus 1 through the impedance can be written:

$$-P_{10} = \frac{V v_1 \cos(\theta_0 + \delta_1)}{Z_0} - \frac{{v_1}^2 \cos(\theta_0)}{Z_0} \quad (2.1)$$

$$-Q_{10} = \frac{V v_1 \sin(\theta_0 + \delta_1)}{Z_0} - \frac{{v_1}^2 \sin(\theta_0)}{Z_0} \quad (2.2)$$

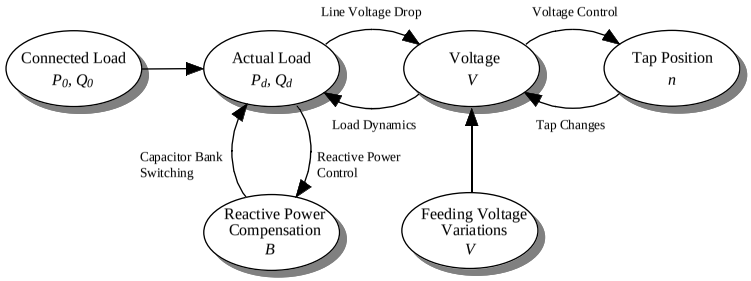

Figure 2.1 Sketch illustrating the couplings between the physical phenomena that create the need for voltage control.

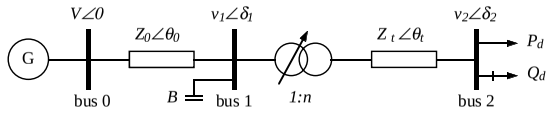

Figure 2.2 A simple model of the distribution system studied.

where V and v_1 are the sending and receiving end voltage amplitudes respectively, and δ_1 the receiving end voltage angle. Given the active and reactive power transport, the receiving end voltage and voltage angle can be numerically computed from Equations (2.1)-(2.2). Figure 2.3 shows the voltage amplitude at bus 1 for different load conditions. The shaded part of the surface corresponds to cases where the sub-station transformers at Tomelilla are operated below their rated limits (100 MVA). The voltage drop increases with increased loading of the line. Also, reactive loading causes a slightly larger voltage drop than corresponding active loading. The voltage drop at the 130 kV bus is about 5-10 % depending on the load power factor when the transformer is loaded to the rated power loading. The capacitor bank has been switched off in the calculations.

Reactive Power Compensation

Reactive power compensation reduces the amount of reactive power transported, and thereby active as well as reactive losses, by generating reactive power close to the reactive load. Long, lightly loaded transmission lines or cables generate reactive power. Therefore excess reactive power sometimes must be consumed by shunt reactors. Reactive power compensation can also

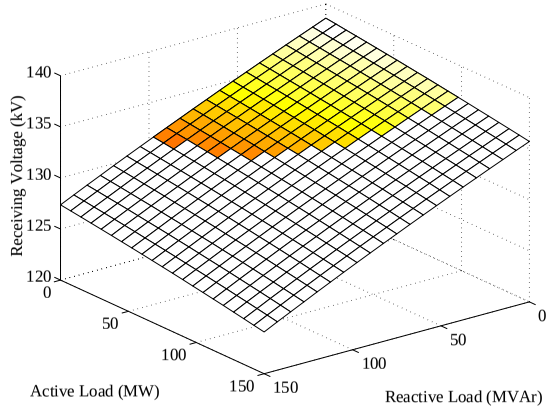

Figure 2.3 Illustration of line voltage drop. The shaded part of the surface corresponds to the loadings below the rated power of the sub-station transformers in the Tomelilla sub-station (100 MVA)

be used to alleviate temporary over- or under-voltages due to disturbances.

Mechanically switched shunt capacitors and reactors are the most common means of reactive power compensation. Lately some power electronic components, like static VAR compensators (SVCs) have been introduced. Their main advantage is that their reactive power output can be varied continuously, as opposed to shunt capacitors and reactors that are operated in fixed steps. Although the primary purpose of an SVC is usually reactive power compensation and rapid control of the voltage at weak points in the network [IEEESVC, 1994], the capability of fast switching also makes SVCs useful for other tasks that require rapid control. Damping of electromechanical oscillations [Lerch et al., 1992] is one example. The connection of a capacitor bank to a distribution bus adds a reactive power injection to that bus, and consequently relieves the supplying system of reactive load, thereby increasing the voltage at that and neighbouring buses. Capacitor banks are usually rated by their reactive power output (MVAr) at nominal voltage rather than their capacitance (F).

Figure 2.4 shows a simulation of the voltage response when 60 MVAr of reactive compensation is switched in at simulation time 100 s. The switching causes an instantaneous voltage increase of about 3 % at the 130 and 50 kV levels. The OLTC regulates the 50 kV voltage and compensates the voltage step. Consequently, the voltage at the 130 kV bus further increases due to the load relief as the load voltage returns to normal.

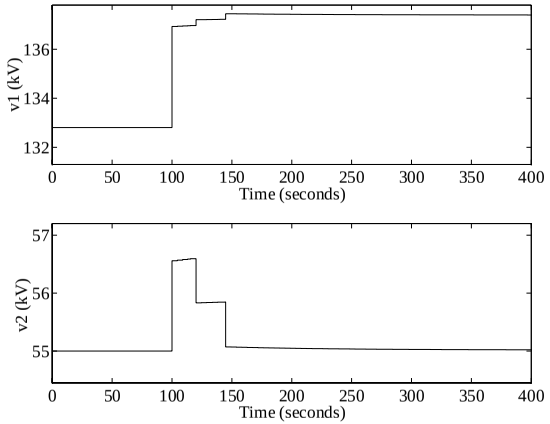

Figure 2.4 Simulation of voltage response to a switching of the 60 MVAr capacitor bank.

Connected Load and Feeding Voltage Variations

The connected load (P_0, Q_0) at a point in the network is the sum of the rated W and VAr of all connected devices below that point. If all load devices are operating in steady-state and supplied at nominal voltage, this is equal to the actual load demand. The connected load varies over the season due to climate variations; over the week due to holiday/working days; and over the day due to daily routines. A curve showing the daily load variations is referred to as a *load curve*.

Figure 2.5 shows the load curve for the 130/50/20 kV transformer in the TLA sub-station for one winter and one summer day. Because of the climate variations in combination with the widespread use of electric space heating, the winter load is substantially larger than the summer load. The daily peak load occurs just before noon. Additionally, the winter curve has a distinct peak around 18 o'clock that is usually ascribed to household cooking [Lakervi and Holmes, 1989]. During weekends and holidays, the load demand is generally lower and the noon peak less distinct due to the lower demand of industrial and commercial load.

The variations of the feeding sub-transmission voltage are closely related to the variations of the connected load because of the line voltage drop. Although there are OLTCs on all Swedish VHV/HV transformers, the 130 kV voltage tends to fluctuate about 4-5 % at TLA during a normal days operation.

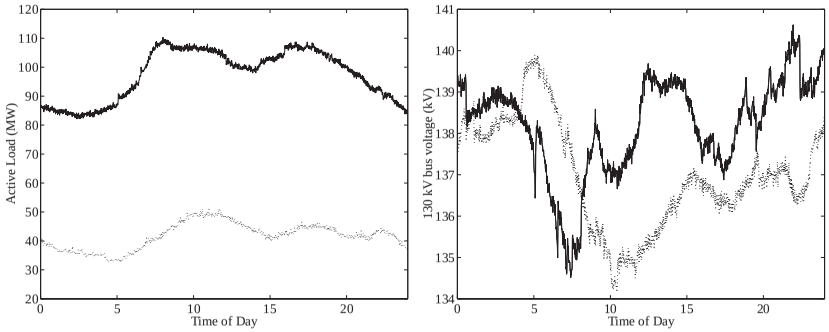

Figure 2.5 Load curves and feeding voltage recorded at the Tomelilla 130/50/20 kV transformer recorded on Thursday, December 21, 1995 (solid curve) and Thursday, July 10, 1996 (dotted curve).

Figure 2.5 shows the voltage feeding the 130/50/20 kV transformer for the summer and the winter case. Although the load variations are larger in the winter, the feeding voltage variations are roughly the same in the winter and the summer. Possible explanations of this are that the (sub-)transmission network is configured to be weaker in the summer than in the winter and that fewer voltage control actions are taken in the transmission system in the summer.

Load-Voltage Dependency

Besides the aggregate load variation due to the connection/disconnection of load devices, most individual load devices have a voltage dependency.

There are two fundamentally different approaches to the modelling of load-voltage dependency. One method is to start from models of the individual load devices and aggregate them according to the load composition below a certain point in the network. The main advantage of this approach is that the load parameters have a physical meaning. Since each load device is physically modelled it is reasonable to assume that these aggregated models are appropriate for large disturbances, provided that the individual component models are appropriate. Drawbacks of this method are the difficulty of knowing the true load composition and the large computational complexity when these models are used for simulation. The other approach employs parameter estimation methods and black-box modelling. Parameter values in a nominal model structure can be mathematically extracted from a recorded load response to a known disturbance. A disadvantage with these

models is that they can only be trusted to be reliable under the same load conditions and for the same type of disturbance as when the recordings were done. Control design on the basis of this type of model would require on-line parameter estimation. Examples of both approaches to load modelling are briefly described in [IEEELoad, 1995].

The load model that is used throughout this thesis was proposed in [Karlsson, 1992] through the parameter estimation approach to load modelling. Load parameter values obtained over a wide range of operating conditions were also given. The model is based on the assumption that most load devices have an instantaneous impedance characteristic, resulting in an instantaneous load relief if the supply voltage decreases. Some loads, for example electric space heating, have control systems causing load recovery after the voltage decrease. Also, the load seen from MV or higher voltage levels most often includes tap changers that aim to restore the load side voltages, and thereby the load, following voltage variations. When the load dynamics are fully recovered and the load is supplied at nominal voltage, the actual load is equal to the connected load. The model structure is:

$$\dot{x}_p = \frac{1}{T_p}(-x_p + P_s(V) - P_t(V)) \tag{2.3}$$

$$P_d = x_p + P_t(V) \tag{2.4}$$

where x_p is an internal state modelling the load recovery dynamics. The active load model is parameterised by the steady-state voltage dependency $P_s(V) = P_0 V^{\alpha_s}$, the transient(instantaneous) voltage dependency $P_t(V) = P_0 V^{\alpha_t}$ and a recovery time constant T_p. P_d is the actual active power load and P_0 is the sum of the rated power of the load connected. A similar model is used for the reactive power, with corresponding characteristics $Q_s(V) = Q_0 V^{\beta_s}$, $Q_t(V) = Q_0 V^{\beta_t}$ and recovery time constant T_q. Typical parameter values are shown in Table 2.1. This model is a special case of the generalised framework for black-box load models presented in [Karlsson and Hill, 1994].

Figure 2.6 shows a simulation of the active and reactive load responses to a 5 % drop in the supply voltage V in the example system. After the disturbance, an instantaneous load response according to $P_t(V)$ and $Q_t(V)$ can be observed. The load then recovers to the values given by $P_s(V)$ and $Q_s(V)$. The 50 kV voltage decreases slightly as a result of the load recovery. The tap changer control system was deactivated in the simulation. Relevant load parameter values are given in Appendix A.1.

On Load Tap Changing Transformers

Most distribution transformers are equipped with a tap changer for regulation of the secondary side voltage. A tap changer is capable of changing the

T_p	T_q	α_s	α_t	β_s	β_t
60-300 s	30-200 s	0-2	1-3	2-5	4-6

Table 2.1 Typical load parameter values.

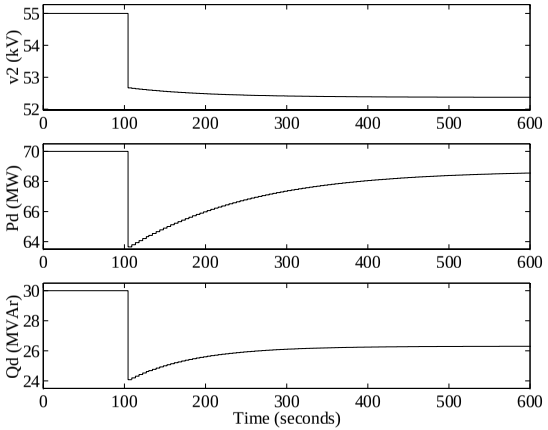

Figure 2.6 Simulation of the load response to a 5% feeding voltage decrease.

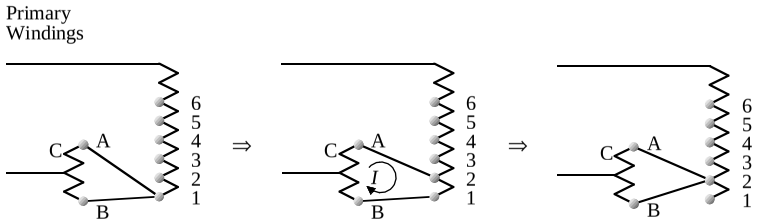

Figure 2.7 The three stages of a tap operation.

number of active turns on one winding of each phase, and thereby adjust the transformer ratio. The tap changer is normally present on the high voltage side since it carries the lower current. The fundamental principle of the tap changer design can be understood from Figure 2.7. Since the tap changer must operate without interrupting the load current, two separate switching arms are used (A, B). The arms are connected to a bridging reactor (C) whose middle point is connected to the primary winding.

In the left figure, illustrating operation at tap step 1, both arms are positioned at connector 1. To make a tap operation to the second step, arm A is first moved to the connector 2 (middle figure) by means of a spring mechanism operated by an electric motor. The voltage between connectors 1 and 2 now creates a circulating current through the bridging reactor and the two switching arms. The purpose of the bridging reactor is to reduce this circulating current. Then, arm B moves to connector 2 and the tap operation is completed (right figure). The turns between connectors 1 & 2 are now bypassed, changing the number of active turns of the primary winding and therefore the transformer ratio. Since the current now flows in opposite directions in the two halves of the bridging reactor, it introduces a negligible reactance. Possible tap ratio change is typically $\pm 10 - 15$ % in steps of 0.6-2.5 %. The mechanical delay time (T_m) is usually in the range 2-5 s (including operation of the spring mechanism). The actual tap operation needs 0.1-0.2 s to complete.

Most tap changer mechanisms are filled with oil for the purpose of insulation. When the switching arms are moved, arcing occurs between the arms and the connectors. The most common reason for tap changer maintenance is degradation of the insulation oil and wear on the connectors and switching arms due to this arcing.

Consider a power transport between buses 1 and 2 in Figure 2.2. The active and reactive power received at bus 2 is given by

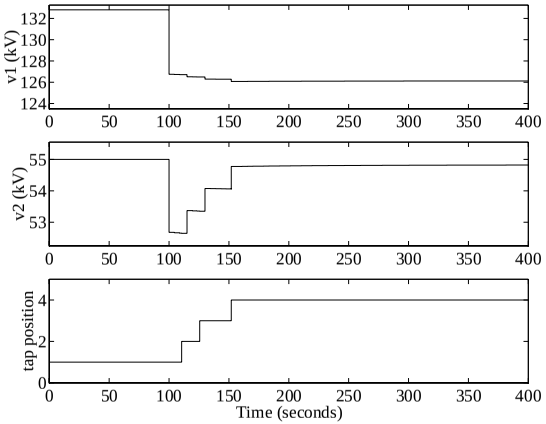

Figure 2.8 Simulation of the OLTC response following a 5 % load feeding voltage disturbance.

$$-P_{21} = \frac{v_1 v_2 \cos(\delta_2 - \delta_1 + \theta_t)}{Z_t n} - \frac{{v_2}^2 \cos(\theta_t)}{Z_t} \quad (2.5)$$

$$-Q_{21} = \frac{v_1 v_2 \sin(\delta_2 - \delta_1 + \theta_t)}{Z_t n} - \frac{{v_2}^2 \sin(\theta_t)}{Z_t} \quad (2.6)$$

where n is the tap ratio. Similarly to the line drop calculation, the receiving end voltage can be calculated numerically from (2.5)-(2.6). Since the effective number of windings is different for different tap positions, a tap dependent transformer impedance is sometimes used, particularly in energy management systems. For study of the voltage control problem, the constant impedance model given by Equations (2.5)-(2.6) is sufficient.

Figure 2.8 shows a simulation of the tap changer response to a 5 % feeding voltage decrease. The tap changer compensates the lowered feeding voltage by making three tap operations. As the tap changer operates, load is restored and the primary side voltage further decreased. The tap changer is controlled by an inverse-time control system (described in Section 3.2).

Besides the conventional (mechanical) tap changer described here, power-electronic tap changers have been considered. They would be capable of high-speed continuous voltage control, without internal arcing. However, the cost of these is presently prohibitively high and they cause substantially larger losses than equivalent mechanical tap changers. Thyristor based OLTCs introduces a harmonic problem, therefore thyristor-assisted OLTCs, in which

the thyristors are used only during tap operations, have been suggested. This enables arc-less but discrete operations with losses on par with equivalent conventional OLTCs. Also they have poor capability of withstanding fault currents [Wood et al., 1988]. Therefore, until significant progress is made in high voltage power-electronics technology, power-electronic tap changers are not likely to be widely used in distribution networks in the near future. When the technology is mature and competitive power-electronic tap changers are available, it will be several decades before all conventional tap changers are replaced. Therefore coordinated tap changer control will not be obsolete within the near future.

2.2 The Österlen Test System

A branch of the distribution system at Österlen (Figure 2.9) was chosen for this study of the coordinated voltage control problem. Österlen is a rural area in the Southeast of Sweden. A preliminary study in the area found considerable interaction among the cascaded tap changers [Karlsson, 1993].

At Tomelilla, there are two 100/100/40 MVA, 130/50/20 kV tap changing transformers. During the winter, both transformers are in use with their control systems operated in a master-slave configuration. To reduce the no load losses, only one transformer is used during the summer. The 50 kV sides of the TLA transformers are connected to three 50/20 kV transformer sub-stations, one of which is Järrestad *(JSD)*, through overhead lines. The tap changers in TLA are placed on the 130 kV windings, and controls the 20 kV voltage. At the 130 kV bus-bar there are one 20 and one 40 MVAr capacitor bank present, making reactive power compensation of 20, 40 or 60 MVAr possible. Since the capacitor banks share a single circuit breaker, with disconnectors determining the amount of reactive compensation used, the capacitor banks cannot be operated in 20 MVAr steps. The switchings of the capacitor banks are therefore a significant disturbance to the voltage control. The capacitor banks are part of the sub-transmission system and are manually controlled from the system operations center in Malmö, usually switched in in the morning and switched out in the evening. For this reason, they are not considered controllable by the voltage control systems in this thesis. The OLTCs in TLA have steps of 1.67 %.

At Järrestad *(JSD)*, one of the two 16 MVA tap changing transformers is normally in operation with the other one as a backup. The JSD station supplies the Östra Tommarp *(ÖTP)* and five other 20/10 kV transformers mainly through overhead lines. The OLTCs in JSD have steps of 2.5 %.

There is one 4 MVA and one 2 MVA 20/10 kV transformer at ÖTP. The 4 MVA transformer is normally in use with the 2 MVA one as a backup. The

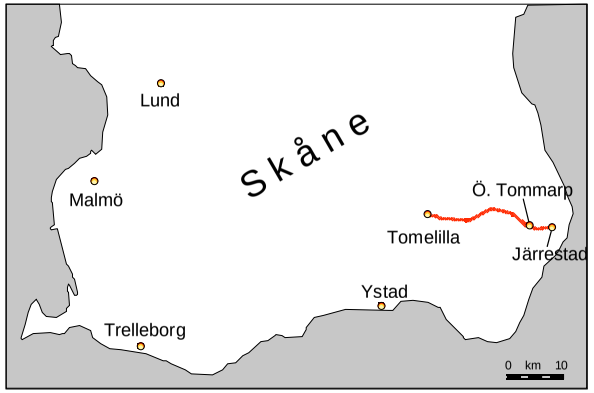

Figure 2.9 Map of the Österlen test area. The thick line denotes the power lines of the branch TLA-JSD-ÖTP.

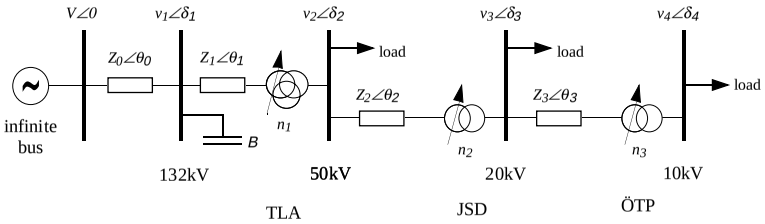

Figure 2.10 Schematic of the test system at Österlen.

ÖTP sub-station supplies 42 10/0.4 kV transformers mainly through overhead lines. These transformers are only equipped with off-load tap changers, and they are not included in the simulation model. The OLTCs in ÖTP have steps of 1.67 %.

Figure 2.10 shows a schematic of the test system with the symbols used in the network model given in Appendix A.1 along with values of the relevant parameters. The 20 kV side of the Tomelilla three-winding transformer is not included in the model and the 20 kV load has therefore been shifted to the 50 kV side in the simulations.

2.3 Voltage and OLTC Control System Stability

Voltage stability has been one of the main research areas of the power system field during the last decades. OLTCs are often referred to as important contributors to voltage instability, since they aim to restore load voltages and thereby load power to the nominal levels even though the transmission system voltages may by low due to severe disturbances. During these extreme operating conditions OLTCs may exhibit a reverse action characteristic such that an upward tap operation might actually yield a lower secondary side voltage, because of the additional strain put on the supplying system. Several studies have suggested tap locking as an emergency action to avoid voltage collapse, for example [Popović, 1995].

Voltage stability is mainly a concern of the transmission system, although local voltage collapse within a distribution system when the transmission system has acceptable voltages is theoretically possible. However, for radial systems without reactive compensation below the OLTCs, the most obvious source of OLTC control system instability is the reverse action phenomena. For the Österlen test system (and possibly Swedish distribution systems in general), the reverse action phenomena requires loading well beyond the rated current limits of the distribution system components to occur. Since the control schemes presented in Chapter 3 are intended for normal-state control, the issue of OLTC control system stability is not addressed there. Studies on the stability of OLTC control schemes have been carried out in [Medanić et al., 1987, Yorino et al., 1996]. Also, Chapter 6 offers some new results on OLTC control system stability.

3

Coordinated Tap Changer Control Schemes

Father, forgive them, for they have not known what they do.

Jesus

This chapter presents the three control schemes considered in the thesis. Using simulations of the Österlen test system in Figure 2.10, the differences between the control schemes are illustrated by simulation of a single days operation. Simulation and measurement results for summer, autumn and winter operating conditions are presented in Chapter 5.

3.1 Demands on Supply Voltage Variation

According to the Swedish standard [SS 421 18 11, 1989], the voltage RMS value shall be within:

$$V_N - 10\,\% < v < V_N + 6\,\% \tag{3.1}$$

for LV networks, where V_N is the nominal voltage. There is no similar standard for the MV voltages, but since there is no direct voltage control at the LV level, the MV voltages must be regulated to keep the LV voltages within acceptable limits. The limits used in this thesis are:

$$-3.5\,\% < v_{dev} < 3.5\,\% \tag{3.2}$$

during normal service conditions for MV networks, where v_{dev} is the voltage deviation from set-point.

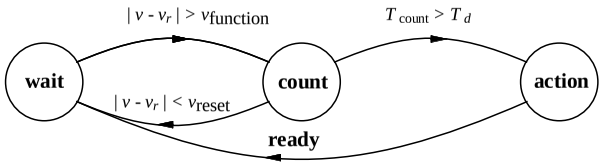

Figure 3.1 State graph illustrating function of a non-sequential OLTC control system.

3.2 Conventional Controllers

An early detailed description of a typical OLTC control system was given in [Ćalović, 1984]. The proposed OLTC model was a complex nonlinear dynamic model that encompassed some inherent time delays. More recent work presented in [Sauer and Pai, 1994] explored further the tap changer modelling issue. Depending on the OLTC characteristic (type of time delay), various discrete state dynamic models and corresponding continuous approximations were derived. The two control systems that are most commonly used in the Swedish system have been modelled in [Altsjö, 1993].

The state graph in Figure 3.1 illustrates the function of a typical OLTC control system. The system remains in the state **wait** as long as the voltage deviation ($|v-v_r|$) is less than the function voltage (v_{function}). When the limit is exceeded, a transition to the state **count** occurs. Upon entering **count**, a timer is started and is kept running until either it reaches the delay time T_d, causing a transition to the state **action**; or the voltage deviation becomes less than the reset voltage (v_{reset}), causing a transition to the state **wait** and reset of the timer. When entering the state **action**, a control pulse to operate the tap changer is given. After the mechanical delay time (T_m), the tap operation is completed and the control system receives a **ready** signal from the tap changer. The control system then returns to state **wait**.

The time delay is tuned by the time delay parameter T_{d0}. The actual time delay can then be either fixed ($T_d = T_{d0}$), or inversely proportional to the voltage deviation ($T_d \sim T_{d0}/|v - v_r|$), depending on the control system.

Constant- versus Inverse-time Characteristics

Two types of time domain characteristics are used in conventional tap changer control systems. The simplest is the constant time variant, where the time delay T_d is constant. With inverse-time characteristics the time delay is dynamically updated according to some formula, for example inversely proportional to the voltage deviation.

Sequential- versus Non-Sequential Operation

This characteristic is only relevant if the voltage deviation is large and more than one tap operation is needed to restore the voltage. With sequential operation, the delay time (T_d) is used only for the first operation. Subsequent operations are ordered immediately and therefore delayed only by the mechanical time delay (T_m). With non-sequential operation the delay time (T_d) is used for all tap steps.

Tuning

The delay time and the function and reset voltages that determine the dead-band are the tuning parameters. The function voltage is usually set slightly smaller than the size of a tap step, to ensure that the voltage will be close to the set-point after a tap operation. For noise rejection purposes, the reset voltage is usually set slightly smaller than the function voltage. The delay time is usually in the range 30-200 s.

Presently, the delay times of cascaded tap changers are tuned to the same value in Sydkraft's distribution networks. Figure 3.2 shows a simulation of the OLTC response to a 5 % feeding voltage decrease with the normal tuning, that is, all three OLTCs has a delay time of 120 s. The dead-bands are tuned according to Table A.1 in Appendix A.1. The three OLTCs compensate the disturbance simultaneously, after 120 s. When the top level OLTC restores its voltage, it introduces a voltage overshoot at the lower level whose OLTC must make a counteracting tap operation. The voltages are restored within their dead-bands using a total of 6 tap operations. Figure 3.3 shows a similar simulation where the top level OLTC has a delay time of 30 s, the middle one has 70 s and the lower one has 150 s. The voltages are restored using 4 tap operations. With the revised tuning, the voltages are restored quicker, with fewer tap operations and without voltage overshoot at the lower level.

Revised Tuning

In Figure 3.3 unnecessary tap operations are avoided by adjusting the time delays. On the basis of this simulation, we can conclude that for step disturbances, no OLTC should act until all higher level OLTCs have compensated for the disturbance. This holds for both load and feeding network step disturbances. A tuning recommendation for cascaded OLTCs in radial networks giving gradually longer delay times for lower level units, is as follows:

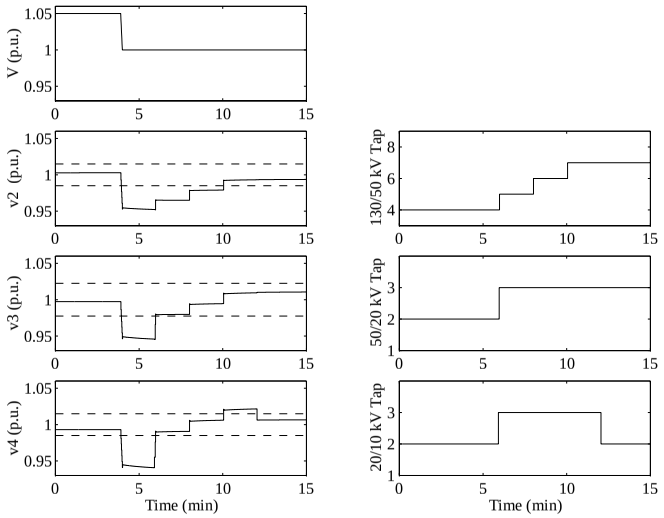

Figure 3.2 Simulation of feeding voltage step decrease. Normal tuning, i.e., all three OLTCs have delay times of 120 s.

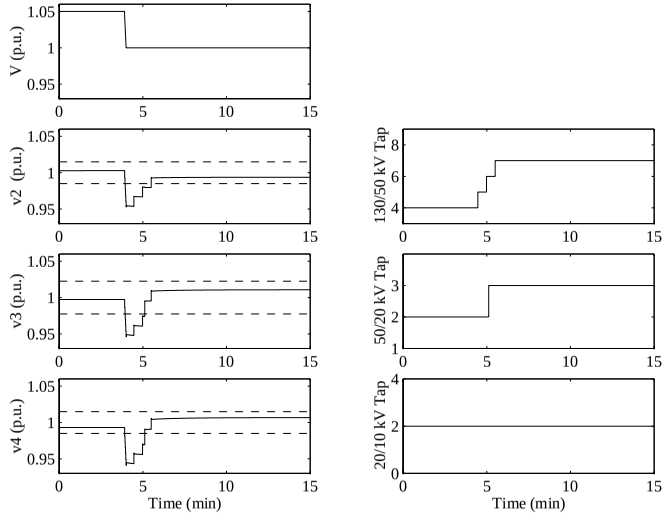

Figure 3.3 Simulation of feeding voltage step decrease. Revised tuning, i.e., the top level OLTC has a delay time of 30 s, the middle one has 70 s and the lower one has 150 s.

1. Set the delay time ($T_{d0,1}$) of the top level OLTC adequately long to filter out fast transients.
2. For a nominal voltage step disturbance at the top level, compute the number of tap operations needed (N) for the top level OLTC to compensate for the disturbance.
3. For lower level OLTCs, make $T_{d0,k+1} > NT_{d0,k} + T_m$.
4. Check that the delay time of the lowest level OLTC provides fast enough customer voltage restoration.
5. Set the lower level OLTCs to operate in non-sequential mode.

The tuning recommendation was first published in [Larsson and Karlsson, 1995] along with extensive simulation results, that show that the revised tuning remain efficient over a wide range of operating conditions. In [Carbone et al., 1996], the authors give a similar tuning recommendation on the basis of voltage stability criteria. The idea of assigning longer time delays to lower level OLTCs is not new, similar philosophies have for long been used by several network operators around the world.

Assuming a disturbance at the 130 kV level of 3 % (this is approximately the voltage deviation created by the connection of capacitor banks at TLA), a delay time of the top level tap changer of 30 s and a mechanical delay time of 10 s, the tuning recommendation yields middle and lower level time delays of 70 and 150 s respectively.

Figures 3.4-3.5 show simulations of a recorded load pattern with the normal and the revised tuning. The control of the top level OLTC is roughly the same for the two tunings, requiring 11 operations in both cases. For the middle level OLTC, there is no interaction with the top level OLTC in the case of revised tuning, whereas with the normal tuning unnecessary tap operations are made at about 7 o'clock and 17 o'clock. The middle level OLTC makes 1 operation with the revised tuning and 5 with the normal tuning. The lower level OLTCs exhibit similar behaviours, resulting in 6 operations for the revised and 15 operations for the normal tuning. There are also fewer voltage spikes due to OLTC interaction in the simulation with the revised tuning, compared to the one with the normal tuning. Some, but not all counteracting tap operations were eliminated in the simulation with the revised tuning.

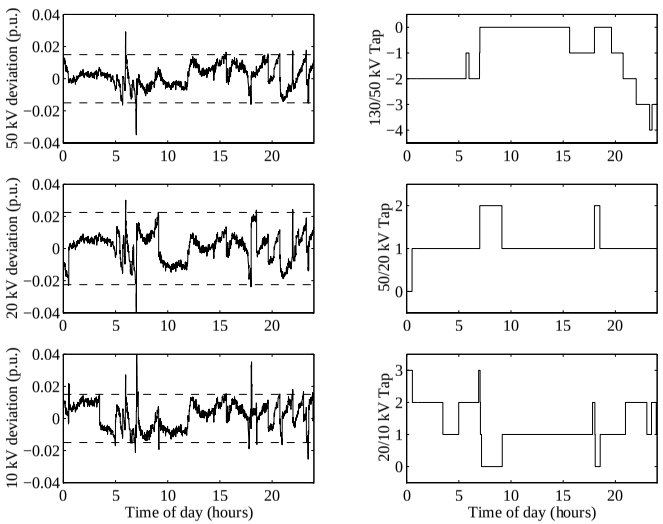

Figure 3.4 Simulation of daily operation. Load pattern recorded October 22, 1996. Conventional control with normal tuning.

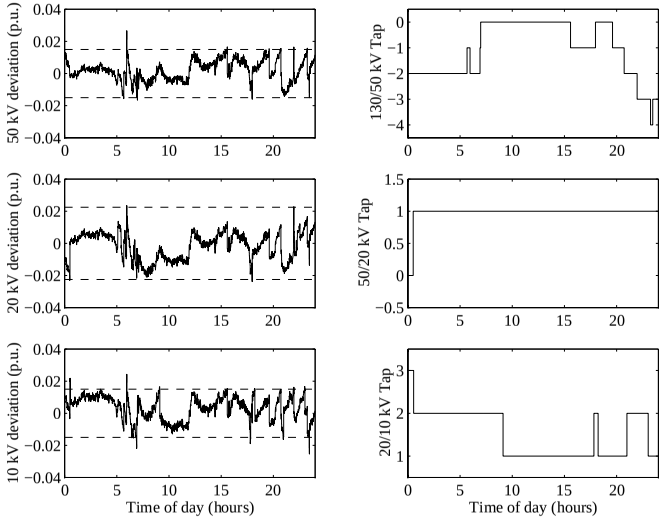

Figure 3.5 Simulation of daily operation. Load pattern recorded October 22, 1996. Conventional control with revised tuning.

3.3 Optimal Controller

In the optimal control scheme the voltage control problem is formulated as a multivariate control problem which is solved by on-line constraint optimisation. Operational limits, such as line capacity limits or tap limits, can be specified as inequality constraints whereas the power-flow equations are specified as equality constraints. The optimisation is dependent on network data.

In this thesis, the optimisation is done statically, that is, only the latest measurements and control signals are considered in the objective function, as opposed to dynamically when control signals are calculated for times up to a prediction horizon based on both old measurements as well as the present. Using a dynamic approach might improve performance further at the cost of a more complex and computationally demanding optimisation. Since static optimisation is used, the controller is optimal in the sense that it gives the optimal tradeoff between voltage deviations and tap operations at each sample, and not necessarily the fewest number of tap operations in daily operation with acceptable voltage deviations. The dynamic approach would also require information about the daily load cycles.

Control Problem Formulation

The coordinated voltage control problem is formulated as the constrained optimisation problem:

$$\begin{array}{lcl} \text{minimize} & : & F(\mathbf{x}) \\ \text{subject to} & : & G(\mathbf{x}) = 0 \\ & & H(\mathbf{x}) \leq 0 \end{array} \tag{3.3}$$

where

$\mathbf{x}$	-	vector of tap positions and auxiliary variables
$F(\mathbf{x})$	-	objective function
$G(\mathbf{x}) = 0$	-	power balance equations
$H(\mathbf{x}) \leq 0$	-	network operational constraints

The auxiliary variables are the voltages from the load flow solution that is obtained at each optimisation step from the solution of the power balance equations. In many ways, this is the same formulation as is used for the Optimal Power Flow problem (OPF). The difference lies in the objective function used. The objective function minimised in the OPF case is based

on network losses, whereas for the OLTC control problem considered here, an objective function based on voltage deviations from set-points and control effort has been used:

$$F(\mathbf{x}) = \sum_i c_i (v_{dev\_i})^2 + \sum_j d_i (\Delta x_j)^2 \tag{3.4}$$

where

v_{dev_i}	-	voltage deviation at bus i
Δx_j	-	change of tap ratio of tap changer j
c_i	-	penalty for voltage deviation at bus i
d_i	-	penalty for operation of tap changer j

Thus, penalties are given for voltage deviations and tap operations in the objective function. Tap changer positions are inherently discretely valued, whereas most optimisation algorithms expect continuous variables. Since tap changer steps are small (0.5-2 %), linear approximation can be used in the optimisation. An alternative would be to use one of the methods that support discrete variables, such as Integer Programming methods and Genetic Algorithms. The Integer Programming method was applied to the coordinated distribution network voltage control problem in [Roytelman et al., 1995]. A Genetic Algorithm was applied to a reactive power optimisation problem in [Lee et al., 1995].

Tuning

The tuning parameters are c_i and d_j by which the desired trade-off between voltage deviations and tap operations can be achieved. The controller was tuned to give roughly the same voltage deviations as the conventional scheme, yielding $c = (1\ 2\ 3)$ and $d = (1\ \frac{1}{2}\ \frac{1}{3})$. Figure 3.6 shows a simulation with the optimal control scheme. In this simulation, the top level OLTCs makes 13 operations, the middle level makes 1 and the lower level makes 3. Whereas retuning of the conventional controllers was not sufficient to remove interaction among the lower level and the other OLTCs, the optimal controller achieves this.

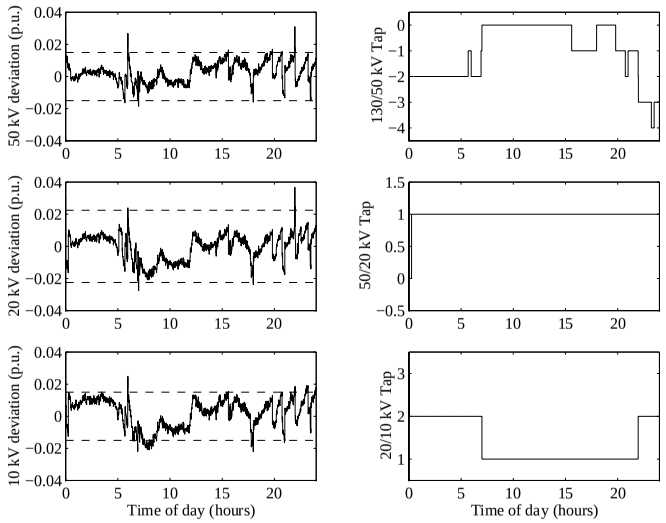

Figure 3.6 Simulation of daily operation. Load pattern recorded October 22, 1996. Optimal control. $c = (1\ 2\ 3)$ and $d = (1\ \frac{1}{2}\ \frac{1}{3})$. The dashed lines show the dead-bands of the conventional control scheme.

3.4 Fuzzy-Rule Based Controller

Introduction to Fuzzy Inference Systems

Fuzzy control has been most successfully used for control problems where the control objectives are difficult to quantify or where one has some heuristic knowledge that can improve control. Instead of using a quantitative model such as the transfer function or state-space models that are the practice in traditional control, one uses a qualitative model formulated as a set of linguistic rules.

The basic idea is that an observation of each physical process variable can be translated to a fuzzy variable giving it a linguistic interpretation. A fuzzy variable has a value between 0 and 1 describing to what extent the observation has the property described by the fuzzy variable. This process is usually called *fuzzification*.

The fuzzy variables can be manipulated with the fuzzy set operators ($\wedge$ (intersection), $\vee$ (union), $\neg$ (complement) etc.) so that combinations of fuzzy variables can be formed and used to determine the controller output. The

mathematics involved in these manipulations are described in [Jantzen, 1991]. They are written as a set of rules on the form:

$$\underbrace{some\ action}_{fuzzy\ controller\ output} = \underbrace{some\ property(\overbrace{some\ variable}^{physical\ variable})}_{fuzzy\ variable} \quad (3.5)$$

The right hand side of (Equation 3.5) may contain several fuzzy variables related by the fuzzy set operations. Together these rules make the *rule-base* of the controller, and should express the heuristic knowledge one has of the system. The process of evaluation of the rules is called *inference*.

The output of the inference is fuzzy variables describing the membership of each controller output to certain fuzzy sets. These fuzzy variables have to be translated to physical controller outputs. This translation is called *defuzzification*.

The entire process can be seen as a mapping, which is often nonlinear, from measurements to controller outputs. Thus, the fuzzy set manipulation in the rule-base is an intuitive way of defining non-linearities for use in feedback control.

Control Problem Formulation

By inspection of results from simulations with the conventional and optimal controller, the following heuristics were formulated:

1. If the voltage is high, order a downward tap operation.
2. If the voltage is low, order an upward tap operation.
3. Cancel an upward tap operation if any tap changer higher up in the network is about to order an upward operation.
4. Cancel a downward tap operation if any tap changer higher up in the network is about to order a downward operation.
5. If voltage deviation is very large, order an operation regardless of rules 3-4.

The next step is to determine which process variables are relevant and define membership functions corresponding to the properties they may possess. Rules 1, 2 and 5 clearly rely on a voltage measurement that can have the properties $very\_low$, low, $high$ and $very\_high$. The corresponding membership functions are shown in Figure 3.7. Since the tap changer in JSD has a larger step size than the other two, it has its own set of membership functions for low and high voltage. No new memberships have to be introduced

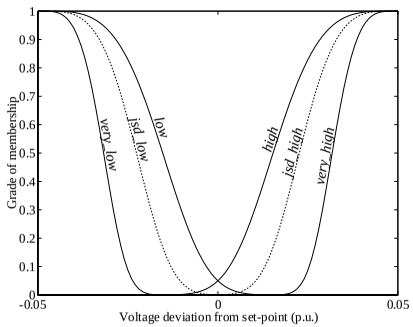

Figure 3.7 Membership functions for voltage deviations.

for rules 3-4, since these rules can be realized using the controller output fuzzy variables UP and $DOWN$ by forward chaining. Using the fuzzy variables and heuristics, the rule base can be formulated:

$$UP_{TLA} = low(v_{TLA}) \vee very\_low(v_{TLA}) \quad (3.6)$$

$$DOWN_{TLA} = high(v_{TLA}) \vee very\_high(v_{TLA}) \quad (3.7)$$

$$UP_{JSD} = (low(v_{JSD}) \wedge \neg UP_{TLA}) \vee very\_low(v_{JSD}) \quad (3.8)$$

$$DOWN_{JSD} = (high(v_{JSD}) \wedge \neg DOWN_{TLA}) \vee very\_high(v_{JSD}) \quad (3.9)$$

$$UP_{OTP} = (low(v_{OTP}) \wedge \neg(UP_{TLA} \vee UP_{JSD}) \vee very\_low(v_{OTP})) \quad (3.10)$$

$$DOWN_{OTP} = (high(v_{OTP}) \wedge \neg(DOWN_{TLA} \vee DOWN_{JSD})) \vee very\_high(v_{OTP}) \quad (3.11)$$

The fuzzy sets UP and $DOWN$ are generated using fuzzified voltage measurements as input for each tap changer. The controller outputs are then determined by defuzzification of the fuzzy sets UP and $DOWN$. The defuzzification is done by subtracting the memberships of UP and $DOWN$, giving a number in the interval $[-1, 1]$ describing to what degree a tap operation should be done and in what direction. The resulting surfaces are called

control surfaces. The control surfaces for the tap changers in TLA and JSD are shown in Figure 3.8. The control surfaces for ÖTP are similar.

Again, because of the OLTC's discrete nature, discretisation of the control surfaces has to be done. In the design, the degree +0.5 is considered enough for an upwards operation and -0.5 enough for a downward operation.

Tuning

Tuning of the rule based controller is done by adjusting the membership functions. The membership functions and the defuzzification threshold has been chosen such that the voltage tolerance given by the first two heuristic rules is roughly the same as for the conventional control (1.5 % in TLA and ÖTP and 2.25 % in JSD gives membership to the degree of 0.5). By adjusting the membership functions for *very_high* and *very_low* the maximum allowable voltage deviations are set to about 3% according to the voltage deviation criterion (3.2). When the heuristic rules 3-4 are active, they specify modifications to the first two rules that cancel operations ordered by rules 1-2, but not those ordered by rule 5. Figure 3.9 shows a simulation of a days operation with the fuzzy rule-based controller. For this particular load pattern, the response is more or less identical to that obtained with the optimal controller.

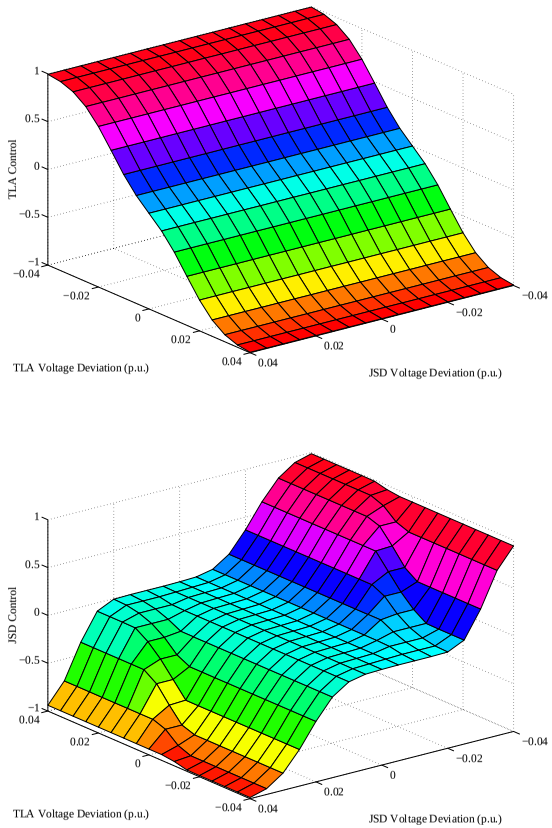

Figure 3.8 Control surfaces

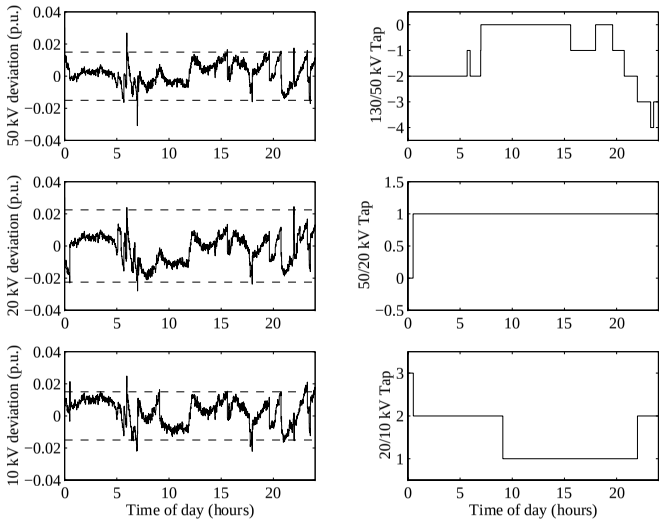

Figure 3.9 Simulation of daily operation. Load pattern recorded October 22, 1996. Rule-based control. The dashed lines show the dead-bands of the conventional control scheme.

3.5 Comparison

All the controllers have been tuned to maintain acceptable voltage variations according to the criterion (3.2). Nevertheless, there is a wide variation in the number of tap operations required. The sequence in which the OLTCs operate greatly affects the total number of operations needed to compensate a disturbance (compare Figures 3.4-3.5). The ability of a control scheme to perform tap operations in correct sequence is here referred to as *selectivity*. The optimal and rule-based controllers offer significantly better selectivity than the conventional scheme, even with the revised tuning. Referring to controller selectivity properties, two different classes of disturbances can be distinguished:

Step or Fast Ramp Disturbances cause the voltage deviation to exceed the dead-band simultaneously for all affected OLTCs. Since the higher level OLTC has the smallest time delay, this reacts to the disturbance before the lower level OLTCs. Thereby reverse tap operations by lower level OLTCs are avoided.

Slow Ramp Disturbances cause voltage change in the same direction for all affected OLTCs. The OLTC whose voltage deviation first exceeds the dead-band reacts first to the disturbance. If this is a lower level OLTC it will have to make reverse tap operations as the higher level OLTCs restore their voltages. The conventional controllers are not capable of providing selectivity for this kind of disturbance, regardless of tuning.

The distinction between slow and fast is here related to the time-scale of the OLTC time delay and step size. Disturbances in the scale of percent per second are definitely fast whereas disturbances in the scale of a less than half a percent per minute can be considered to be slow. A typical source of step disturbances is the variation of the feeding voltage due to switching of capacitor banks or lines in the transmission system. Fast ramp disturbances may occur due to generator voltage control. Slow ramp disturbances occur due to the daily load variations.

The properties of the optimal and rule-based controller differ in that the rule-based controller provides only one-way selectivity, in that an OLTC is controlled only on the basis of its own voltage deviation and those of higher level OLTCs. The optimal control scheme always uses all voltage deviations, thereby providing two-way selectivity. A qualitative difference that arises from this is that the optimal control scheme sometimes allows voltage deviations at higher voltage levels, in order to save operations on the lower levels.

The conventional control scheme is not suitable for meshed networks where transformers are connected in parallel because of the circulating reactive currents and unstable voltage control that might arise [Lakervi and Holmes, 1989]. The optimal control scheme can be used for meshed networks as well, if a term proportional to system losses in (3.4) is added. Similarly, the rule-based control can be augmented with rules to balance the reactive power transport through lines and transformers connected in parallel.

We see that the optimal controller has a number of drawbacks that make it impractical for actual implementation. Perhaps the most serious one is that it is a pure feed-forward controller, using only measurements of the disturbances and compensating for them. Thus, a perfect network model is necessary to regulate voltages without stationary control error. Since network impedances change, most drastically due to switchings in the network but also due to temperature, the optimal controller must be supplied with up-to-date information about network impedances in an actual implementation. This will be possible in the future when DA is widely implemented, but in this thesis the optimal controller has been used mainly as a benchmark for the rule-based controller. The computational complexity is not a major drawback, since distribution systems are typically of moderate size (< 50 OLTCs), and the results from the previous time-step can be used as a very good initial guess in the optimisation. The properties of the three control schemes can be summarised as follows:

Conventional Control with Revised Tuning

+ preserves the existing controllers
+ local control system, no need for communication
+ robust, no network model needed
+ relies only on voltage measurements
- no selectivity for ramp disturbances
- suitable for radial network operation only
- slow customer side voltage restoration

Optimal control

+ excellent selectivity properties
+ fast customer side voltage restoration
- pure feed-forward controller, need for accurate network model
- need for measurement of load powers
- centralised, dependent of communications

- computationally demanding

Fuzzy Rule-based Control

+ very good selectivity properties
+ intuitive because of the rule-base design
+ robust, no network model needed
+ relies only on voltage measurements
+ computationally simple
- centralised, dependent of communications

4

Prototype

The difference between theory and practice is much greater in practice than in theory.

Dr. Jeff Case

To validate the simulation results and to demonstrate the implementation of the coordinated control schemes, a prototype controller was developed and installed in the test system at Österlen. It is a distributed control system, with a local control loop in each sub-station. A supervisory controller in the TLA sub-station coordinates the local control loops, with the necessary communication between the sub-stations provided by radio links. The radio links are driven by standard modems with *RS-232* interfaces. Since the local control loops were implemented using LonWorks components, this chapter starts with an introduction to the LonWorks system.

4.1 LonWorks

LonWorks [LRG, 1992] is a tool for solving distributed control problems. A LonWorks network has no central control or master-slave architecture. Intelligent control devices and sensors, called nodes, communicate with each other using the LonTalk protocol on a peer-peer basis. Each node typically has a simple task, like measurement or control of an actuator. The nodes communicate using the LonTalk protocol, which implements all the seven layers of the OSI model [Stallings, 1991]. Since the protocol was designed with control applications in mind, it is optimised for use with large quantities of small data packets.

There are many manufacturers of standard LonWorks nodes for specific functions and custom nodes can be programmed in Neuron C, a C dialect

with an additional real-time kernel, using the LonBuilder development tool. The concept of *network variables* is one of the unique features of the Neuron C language. When a variable is declared as a network variable, it is made part of the node's external interface and can be connected to other nodes. If it is an output variable, the node is referred to as a producer node (as opposed to consumer node if it is an input variable). When the producer makes a change to the variable, all consumers are notified of the change. The necessary communication is automatically taken care of by the operating system. The neuron chip has a rather limited memory area for user applications and their tasks have to be relatively simple. Complicated applications can be implemented in a PC and interfaced to the LonWorks network through for example a serial interface. The LonBuilder development tool with the Neuron C compiler and the LonMaker installation tool can be used with a standard 486 PC (or better). Some of the most important components are described below:

The Neuron Chip is the core component of any node. It is a chip that internally consists of three microprocessors, two of which handle the communication with other nodes. The third processor executes the node application program. This processor has a clock frequency of 10 MHz, making it computationally on par with the first generation of PC's. There is also an assortment of memory: ROM that stores the operating system and EEPROM and RAM for application execution and storage. The EEPROM memory area can be used to ensure a safe startup after a program crash or a power outage. The Neuron Chip [1] is manufactured by Motorola and Toshiba.

Transceivers are connecting circuitry for communication on a physical network. Several versions are available for different media.

Routers are special nodes used to connect two or more local networks. References to nodes outside the present network are automatically forwarded to the correct subnetwork. Different media may be used on either side of the router.

4.2 Prototype Controller

The controller was implemented with one local LonWorks network in each sub-station, with radio links connecting the local networks. There are separate nodes for OLTC control, measurement and communication with the

[1] The Neuron Chip has absolutely nothing to do with neural networks!

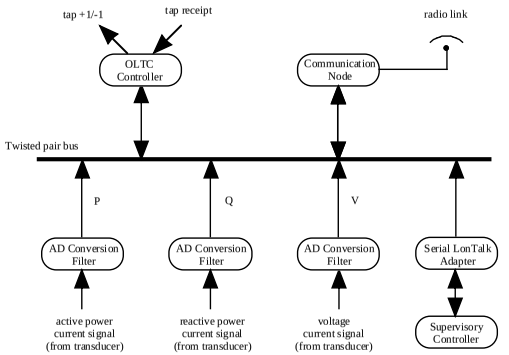

Figure 4.1 Schematic of the local network at TLA

other sub-stations in each sub-station. The supervisory controller was implemented in a 486 DX4 PC in the TLA sub-station.

Figure 4.1 shows a schematic of the local network in the TLA sub-station. The nodes communicate using network variables and the *TP-78* bus within the sub-station, and with nodes in other sub-stations through the communication node and the radio-link.

The TapTalk Protocol

The LonTalk protocol could not be used for the communication over the radio links, since no LonTalk/RS-232 router was available when the implementation phase was initiated. Instead, the TapTalk protocol which implements the three lowest layers of the OSI model was constructed. TapTalk communication is more efficient than the corresponding LonTalk communication although neither as flexible nor reliable. TapTalk is a packet-switching protocol, and the Neuron C header file for the protocol, where the packet data type (**messageType**) is defined, is present in Appendix A.3.

The Physical Layer interfaces to the physical communication medium. It provides a point-to-point channel with synchronisation, flow control and limited error checking using a parity bit for data blocks (bytes) using the RS-232 standard.

The Data Link Layer provides a safe point-to-point channel for streams of data blocks. The data blocks provided by the Data Link layer are assembled into data packets. When a packet is sent, an 8 bit CRC

is piggy-backed on the packet for error checking. Upon receiving a package, the receiver computes a checksum and compares it to the one received with the packet. If it is correct, an acknowledge signal is sent to the sender node, or the receiver node requests retransmission of the package. This process is repeated until the transmission succeeds or a retry limit is exceeded.

The Network Layer provides a channel between different networks. This layer deals with routing of data packets to the correct network.

Since the protocol was designed specifically for use with the coordinated voltage controller, a rather low communication speed of 600 bps could be used for the radio link.

Communication Nodes

The communication nodes have four separate tasks:

Inter-station Communication
Exchange of measurements and control signals with the central controller over the radio links using the TapTalk protocol.

Execution of commands
When commands are received through the radio link they are forwarded to the correct node in the local network. For example, when a packet consisting of a remote control signal arrives, the communication node orders the OLTC controller node to make a tap operation. In a periodic way, presently every 10 seconds, packets with up-to-date measurements are sent to the Tomelilla sub-station. The communication node also forwards messages to other stations.

Conditioning of Measurements
The Analog Input Nodes provides current measurements from the measurement transducers. These are translated into the p.u. quantities used by the control system by the communication node. In the Tomelilla station, the load power measurements are conditioned by the supervisory controller to relieve the communication node of computational load.

Safety Net
Each time the communication node receives instructions from the central controller, a count-down timer is started. If the timer expires, the communication node assumes that it has lost contact with the supervisory controller and orders the OLTC control node into local control mode. Also, if the voltage deviation exceeds 5% for more than five

minutes, the supervisory controller is assumed to be malfunctioning and the OLTC control node is ordered into local control mode.

OLTC Controller Nodes

The OLTC controller nodes implement control systems according to section 3.2 operating in constant-time non-sequential mode (local control mode). In addition, they can be remote controlled from the supervisory controller with absolute or incremental control signal (remote control mode). Normally the node operates in remote control mode, but whenever contact with the supervisory controller is lost or it is malfunctioning the OLTC controller nodes enter local control mode. The OLTC controller node also contains logic for slave-controlling a second transformer operating in parallel with the main transformer on the basis of a reactive power balancing criterion. The tuning parameters for the local control mode is set using the LonMaker installation tool.

Analog Input Module

Standard modules from Weidmüller were used as analog input nodes. These modules perform analog-digital conversion of and filters the current measurements received from the measurement transducers.

LonWorks DDE Server

The LonWorks DDE Server is manufactured by the Echelon Corporation, and gives access to the network variables via the *Dynamic Data Exchange (DDE)* functions available in Windows 3.11. The DDE Server is a piece of software executing in the PC. The PC is connected to a *Serial LonTalk Adapter (SLTA)* through the serial port. The SLTA is also connected to the LonWorks networks. Up-to-date measurements are cached in the DDE Server to provide rapid access from DDE Clients.

MATLAB DDE Server

The control algorithm was implemented in MATLAB. In the Windows 3.11 version, MATLAB is capable of acting as a DDE server. With a sampling time of one minute, measurements are received from the supervisory controller and control signals are updated. Since the simulations were also done with MATLAB, exactly the same code can be used in the prototype.

Supervisory Controller

The supervisory controller was programmed using InTouch, a generic tool for construction of user interfaces. Every minute it sends new measurements to

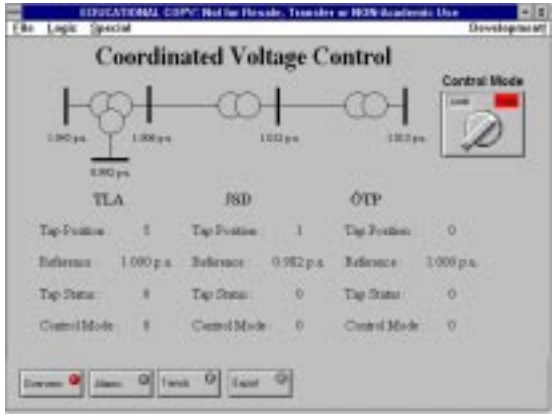

Figure 4.2 The overview display.

the MATLAB DDE Server and receives updated control signals. The control signals are then passed on to the LonWorks DDE Server that forwards them to the correct OLTC controller. The supervisory controller is also responsible for logging of measurements and alarms.

Figure 4.2 shows the overview screen where the voltage control can be monitored and the control mode can be switched between conventional or fuzzy rule-based control. Figure 4.3 shows the alarm history screen where the events that have taken place are reported. Examples of reported events are violation of alarm limits, communication failure and change of control mode. Two types of display are available, a summary display where alarms are displayed until acknowledged or a historical display where all alarms are shown with time of acknowledgement. Figure 4.4 shows the trend display where historical data can be plotted. Old measurements are stored in a database on the PC's disk, and can be retrieved by specifying the time range of the plot. The export display shown in Figure 4.5 can be used to export historical measurement and alarm data through a DDE channel.

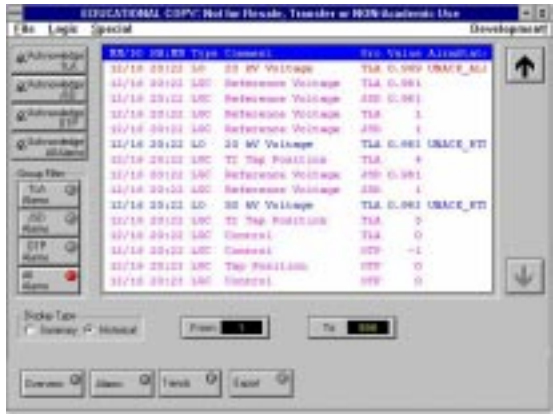

Figure 4.3 The alarm log.

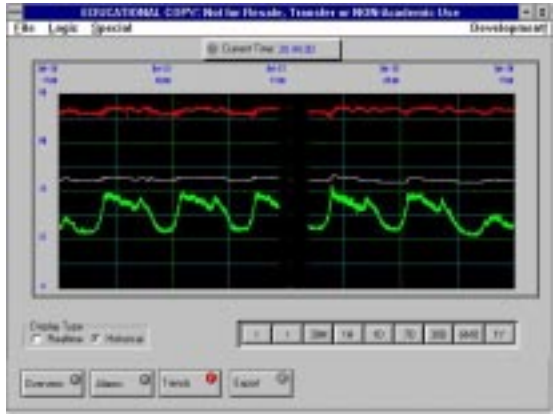

Figure 4.4 The historical trend display.

Figure 4.5 From within the supervisory controller, measurements and alarms can be exported through a DDE channel.

5

Simulation and Field Test Results

My opinions may have changed, but not the fact that I am right.

Ashleigh Brilliant

5.1 Load Pattern Recordings

To be able to compare the control schemes using realistic load patterns, the prototype was used to record the load variations at TLA, JSD and ÖTP and the feeding 130 kV voltage at TLA during three two-week measurement periods:

Summer: July 10-16 and July 21-27, 1996.

Autumn: October 16-22 and 24-30, 1996.

Winter: January 13-26, 1996.

The local control scheme was in use during the summer, winter and first week of the autumn measurement. The fuzzy-rule based controller was in use during the second week of the autumn measurement.

5.2 Simulation Results

Figures 5.1-5.3 show the daily average number of tap operations and the voltage standard deviations observed in the simulations with the four control

schemes. The control schemes were tuned according to Chapter 3 and are abbreviated as:

- conventional control scheme with normal tuning *(CCN)*
- conventional control scheme with revised tuning *(CCR)*
- fuzzy-rule based control scheme *(FRB)*
- optimal control scheme (*OPT*)

The voltage deviations are about the same for all controllers, so that the control schemes can be justly compared in terms of the daily number tap operations required.

Variations with Respect to Control Scheme

The variation with respect to the control scheme is the most important factor to consider. The total number of tap operations per day averaged over the three periods are summarised in table below:

	CCN	CCR	FRB	OPT
Number of operations	27	24	15	13
Compared to CCN		-3	-12	-14
Relative to CCN (%)		-10 %	-43 %	-51 %
Compared to CCR			-9	-11
Relative to CCR (%)			-36 %	-45 %
Compared to FRB				-2.1
Relative to FRB (%)				-14 %

Seasonal Variations

As can be expected, there is a clear variation in the number of tap operations over the three measurements. The table below summarises the simulation results averaged over the three periods and four control schemes:

	Summer	Autumn	Winter	Average
Number of operations	13	19	22	18
Compared to average	-5.1	+0.9	+4.2	-
Relative to average	-29 %	+5 %	+24 %	-

The increased number of tap operations observed in the winter measurement is a direct result of the larger variation of the connected load. The

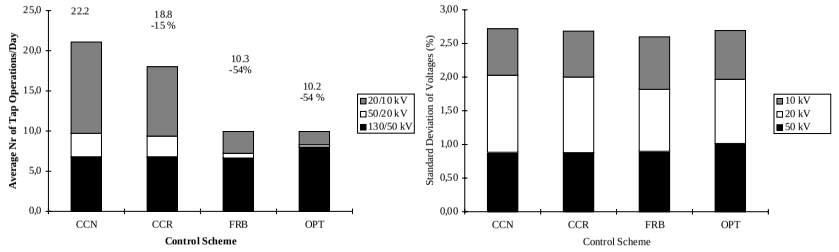

Figure 5.1 Simulation results. Load patterns recorded during the summer measurement.

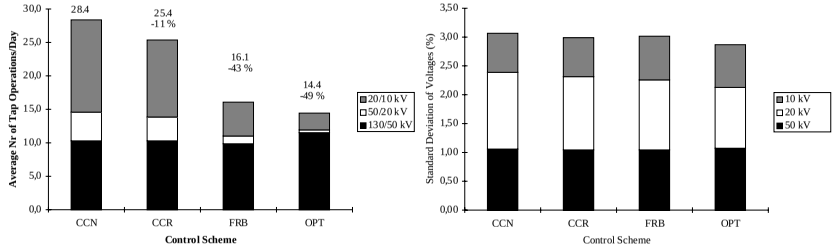

Figure 5.2 Simulation results. Load patterns recorded during the autumn measurement.

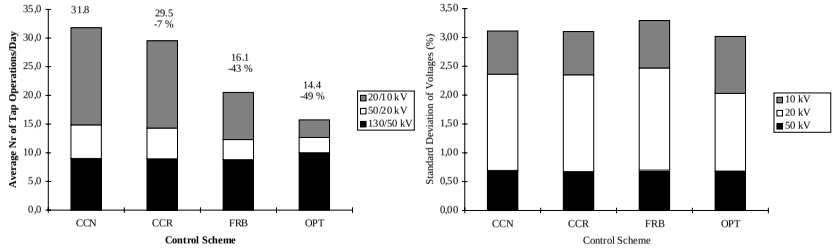

Figure 5.3 Simulation results. Load patterns recorded during the winter measurement.

relative saving with the CCR is larger the summer (-15 %) than in the winter measurement (-7 %). A possible explanation for this is that the number of operations due to step-disturbances, for which the CCR provides selectivity, that occur daily is fairly constant over the seasons, whereas the number operations due to ramp-disturbances increases during the winter measurement because of the higher load level. Similarly, the performance of the FRB is at its best during the summer measurement where it uses about the same number of operations as the OPT. In the autumn and winter measurements, its performance is not as good as that of the OPT but still considerably better than those of the CCR and CCN.

Variations by OLTC level

The table below summarises the daily number of tap operations obtained by simulations averaged over the three periods:

	CCN	CCR	FRB	OPT
130/50 kV	8.7	8.7	8.4	9.8
Relative to CCN		0 %	-3 %	+13 %
50/20 kV	4.4	3.8	1.8	1.1
Relative to CCN		-12 %	-60 %	-74 %
20/10 kV	14	12	5.3	2.4
Relative to CCN		-16 %	-62 %	-83 %

Since the control of top-level OLTC is similar for all control schemes, the variation in the number of operations made by this OLTC is small. The most distinctive difference is that the OPT tend to use more operations at the top level, in order to save operations at the middle and bottom levels. The large savings are made at the middle and bottom level for all the new control schemes.

5.3 Validation

The simulation results were validated during the autumn measurement period. The CCN was in operation during the first week and the FRB during the second. Figure 5.4 shows a comparison of the average number of tap operations during the validation measurement. To the left, simulation results for the two weeks can be compared for the different control schemes. The conclusion that can be drawn, is that the overall number of operations tends to be slightly larger during the first week. The two rightmost bars show the

number operations observed in the measurements, with the CCN during the first week and the FRB during the second week. This measurement supports the simulation results, since the observed reduction by the FRB compared to the CCN, is about 60 % while the simulations indicates a 59 % reduction. Figure 5.5 shows the voltage standard deviations, which are more or less the same in the measurements and simulations.

It is also interesting to look at the time response to make a visual assessment of the agreement between simulations and the measurements. Figure 5.6 shows the measured and simulated time response during a days operation. Clearly, the simulated response does not perfectly match the measured response. Possible sources of the disagreement are:

- the OLTCs sometimes make two operations when one is ordered
- the OLTC in TLA is sometimes manually controlled from the system operation center in Malmõ
- uncertainty in the network impedances
- uncertainty in the offset of the OLTC ratio
- in practice, the transformer varies with the tap position, whereas it is modelled as a constant impedance in the simulations

However, the differences tend to even out over a longer period of time as seen in Figures 5.4-5.5 in which the simulation and measurement results agree very well. Also, it can bee seen in Figure 5.6, the responses match qualitatively – the slope of the voltage curves and the tolerance for voltage deviations are almost the same in measured and the simulated response.

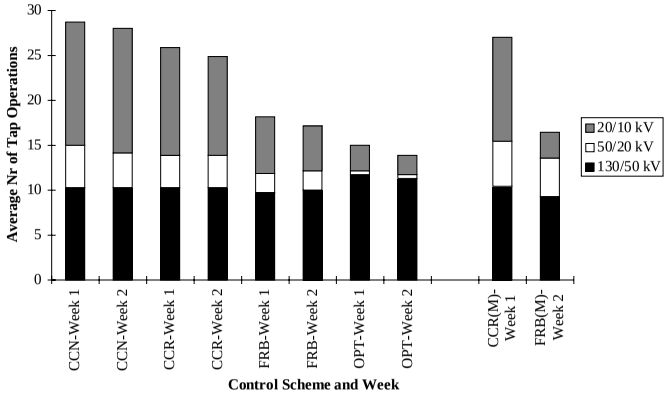

Figure 5.4 Average number of tap operations during the autumn validation measurement. CCR(M) and FRB(M) denotes measurement results with the CCR and FRB respectively.

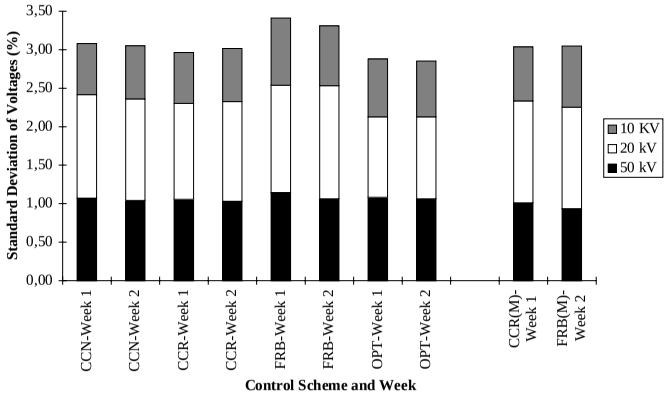

Figure 5.5 Voltage standard deviations during the autumn validation measurement. CCR(M) and FRB(M) denotes measurement results with the CCR and FRB respectively.

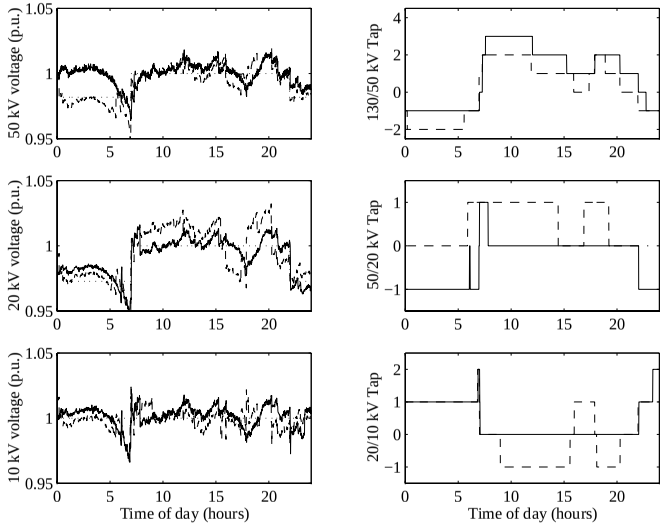

Figure 5.6 Comparison of simulated and measured time response. Simulation (dashed), measurement (solid) and voltage reference value (dotted). Recording done October 25, 1996.

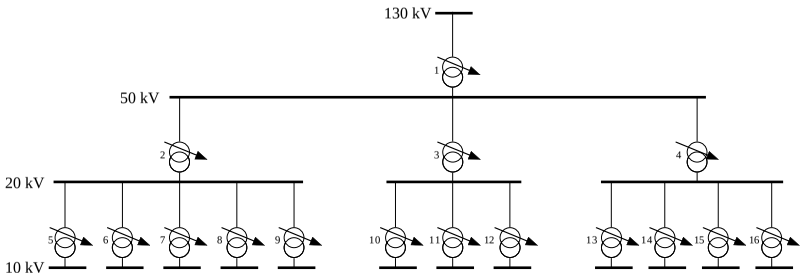

Figure 5.7 Structure of the full distribution system simulated.

5.4 Results for a Full Distribution System

The development of the new controllers has been done using a three tap changer test system. An actual distribution system is successively branching into a large number of nodes at the lower voltage levels. Thanks to the radial topology of the networks, giving weak coupling between different branches, the controllers should work for the entire network as well.

To demonstrate this, a simulation of a fictitious but realistic rural system whose structure is shown in Figure 5.7 was done. Network impedances and load curves for the different voltage levels have been slightly varied around the parameter values for the smaller test system (Table A.1). The results from the simulation are summarised in the table below, with the number of tap operation averaged for each voltage level:

	CCN	CCR	FRB
130/50 kV	8.0	8.0	8.0
Relative to CCN		0 %	0 %
50/20 kV	11.7	9.3	3.0
Relative to CCN	0.0	-20 %	-74 %
20/10 kV	12.6	7.2	3.5
Relative to CCN		-43 %	-72 %
Total	32.3	24.5	14.5
Relative to CCN		-24 %	-55 %

The results from these simulations are similar to those for the smaller test system. Note however, that these results are based on a single days operation, and therefore not as reliable as those presented for the smaller test

system. The lower-level taps, for which the largest savings are done, are the most most numerous in a full distribution system. Since the results in the table are averaged over each voltage level, this is not reflected here. Also, when the coordinated control is implemented in a whole distribution network, some of the 50 kV and 20 kV buses need not necessarily be accurately voltage controlled since they have no loads directly connected. This additional freedom has not been exploited in the simulations, but will possibly reduce the number of tap operations made further.

5.5 Summary of Results

- the results have been obtained using a representative choice of load patterns ranging over 14 summer, 14 autumn and 14 winter days.
- the control schemes have been tuned to give the same voltage standard deviations
- the reduction in terms of number of daily tap operations achieved by the CCR is about 10 % compared to the CCN
- the reduction achieved by the FRB is about 43 % compared to the CCN and 36 % compared to the CCR
- the reduction achieved by the OPT is about 51 % compared to the CCN, 45 % compared to the CCR and 14 % compared to the FRB
- the savings are made at the second and third layer of OLTCs, the number of operations at the top level remains the same
- the simulations have been validated by a field test in the test system at Österlen
- it has been demonstrated by simulations that the CCN and FRB work in a full distribution system

6

On Dynamic Modelling of OLTCs

Celestial navigation is based on the premise that the Earth is the center of the universe. The premise is wrong, but the navigation works. An incorrect model is often a useful tool.

Kelvin Throop III

6.1 Introduction

Studies of serious contingencies and associated voltage instability problems during the past decade have revealed different mechanisms underlying those events. Voltage misbehaviour has been shown as not necessarily just monotonic, influencing researchers to investigate various potential sources of the system oscillatory behaviour. This chapter further explores the oscillatory behaviour of power systems with emphasis on illustrating interactions between on-load tap changer (OLTC) and load dynamics.

OLTCs have been shown to play an important role in long term voltage collapse [Walve, 1986], since they aim to keep load voltages and therefore the load power constant even though transmission system voltages may be reduced. Considerable effort has been given to voltage behaviour research indicating that the dynamics of voltage collapse are closely linked to dynamic interaction between the OLTCs and loads. It led to significant progress in the area of dynamic load modelling. However, most of the power system dynamic studies so far have used quite simplified OLTC representations. The main focus of these studies which mainly relate to voltage stability questions has

been on understanding of the complex dynamic nature of voltage collapse to which OLTC dynamics significantly contributes. The role of OLTCs in combination with aggregate loads has received considerable attention [Abe et al., 1982, Liu and Vu, 1989, Medanić et al., 1987, Popović et al., 1996b, Vu and Liu, 1992]. Voltage instability problems concerned with OLTC dynamics were analysed in [Abe et al., 1982, Liu and Vu, 1989, Popović et al., 1996b, Vu and Liu, 1992] using the continuous state OLTC model. Stability conditions providing proper coordination of multiple OLTCs were derived in [Medanić et al., 1987, Yorino et al., 1996] using a discrete state tap model. Limit cycles and other oscillatory voltage instability problems created by interaction between cascaded tap changing transformers and/or by load-tap interaction were investigated in [Hiskens and Hill, 1993, Popović et al., 1996a, Vournas and Cutsem, 1995].

In this chapter, the influence of OLTC modelling in power system loaded close to oscillatory voltage instability is investigated. The OLTC dead-band is shown to play a central role in creating a limit cycle phenomenon. Using the describing function method, the conditions for this phenomenon to appear is derived.

6.2 Example System

A single load, single OLTC system such as shown in Figure 6.1 is considered. The example system represents a distribution bus fed through a tap changing transformer and a transmission system equivalent. To increase transfer limits, the distribution system has been compensated by a capacitor bank. Although simple, the system contains all the principal components which affect voltage behaviour, especially after line fault or under heavy load conditions.

Load and Network Models

Focusing on tap changer dynamics and therefore on a slower time scale (below ~ 0.1 Hz) than the one relevant to generator dynamics, the generator bus is modelled as an infinite bus. The load is modelled as an exponential recovery load according to equations (2.3)-(2.4), except that $P_s(v) = kP_0v^{\alpha_s}$, $P_t(v) = kP_0v^{\alpha_t}$, $Q_s(v) = kQ_0v^{\beta_s}$ and $Q_t(v) = kQ_0v^{\beta_t}$. The parameter k has been introduced as a scale factor on the load parameters P_0, Q_0 and B_0.

Combining the load dynamics with power balance equations at the load bus, the model can be written in the differential-algebraic form

$$\dot{x} = f(x, V) \tag{6.1}$$
$$0 = g(x, V, n) \tag{6.2}$$

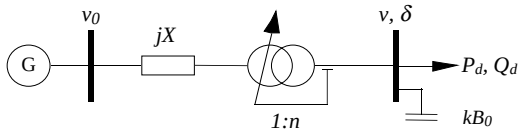

Figure 6.1 Example power system studied.

Network Data	X	B_0	Load Data	P_0	Q_0	T_p=T_q	α_s=β_s	α_t=β_t
	0.5	0.5		1.0	0.5	60	0	2

OLTC Data	tap step	tap limits	DB/2	T	T_{d0}	T_{m0}
	1%	± 15%	0.9 %	30	25*(1/0.9)	5*(1/0.9)

Table 6.1 Network, Load and OLTC Parameter values

where $x = [x_p \ x_q]^T$ is the load state vector, $V = [v \ \delta]^T$ is the load voltage vector and n is the transformer tap ratio. For the example system, functions f and g can be written as

$$f(x, V) = \begin{bmatrix} \frac{1}{T_p}(-x_p + kP_0(v^{\alpha_s} - v^{\alpha_t})) \\ \frac{1}{T_q}(-x_q + kQ_0(v^{\beta_s} - v^{\beta_t})) \end{bmatrix} \tag{6.3}$$

$$g(x, V, n) = \begin{bmatrix} \frac{vv_0 \sin(\delta)}{Xn} + x_p + kP_0v^{\alpha_t} \\ \frac{v(v - \cos(\delta)v_0 n)}{Xn^2} + x_q + kQ_0v^{\beta_t} - kB_0v^2 \end{bmatrix} \tag{6.4}$$

OLTC Models

For the purpose of studying the limit cycling phenomenon, the following three OLTC models will be used:

ODE This is a model where the OLTC is modelled by an ordinary differential equation which is often used in voltage stability analysis. It approximately describes the dynamics of an OLTC with an inverse-time delay characteristic, but does not account for the dead-band or discrete tap steps. The model can be written as

$$\frac{dn}{dt} = -\frac{1}{T}(v - v_r) \tag{6.5}$$

where v is the regulated voltage, v_r is the voltage set-point and T is the controller time delay.

DBODE Augmenting the *ODE* model with a dead-band on the input we get

$$\frac{dn}{dt} = \begin{cases} -\frac{1}{T}(v - v_r - DB/2) & \text{if} \quad v - v_r > DB/2 \\ -\frac{1}{T}(v - v_r + DB/2) & \text{if} \quad v - v_r < -DB/2 \\ 0 & \text{if} \quad |v - v_r| < DB/2 \end{cases} \tag{6.6}$$

where DB is the size of the dead-band.

Detailed is the control system described in Section 3.2 with $T_d = \frac{DB\ T_{d0}}{2|v-v_r|}$ and $T_m = \frac{DB\ T_{m0}}{2|v-v_r|}$.

For agreement with [Sauer and Pai, 1994], function and reset voltages have been chosen to be identical ($u_{\text{function}} = u_{\text{reset}} = DB/2$). It is shown in [Sauer and Pai, 1994] that if T in (6.5) is chosen such that $T\frac{DB/2}{tap\ step} = T_{d0} + T_{m0}$, the *ODE* model makes the best continuous state match to the *Detailed* model in the sense of time response.

To illustrate potential differences in OLTC responses (Figure 6.2), a 5 % disturbance in the feeding voltage, v_0, is assumed in the moderately loaded ($k = 0.5$) power system of Figure 6.1. System parameter values are given in Table 6.2. With the *ODE* model, the tap ratio is adjusted until the voltage deviation becomes exactly zero. Since at that time, the load dynamics have not settled yet, there is a slight overshoot. With the *DBODE* model, the feedback path is broken as soon as the voltage deviation is within the dead-band. Therefore overshoot due to the load dynamics is avoided. With the *Detailed* model, the tap state is changed in fixed steps. Additional voltage restoration due to load dynamics following the last tap operation is also present with this model.

Despite the slight differences in responses in Figure 6.2, the overall behaviour of the moderately loaded system is similar for all OLTC models. The sensitivity to the OLTC modelling is however more significant in a heavily loaded power system. As it will be shown in the following sections, the occurrence of voltage collapse or limit cycles is greatly affected by the OLTC model used in the analysis.

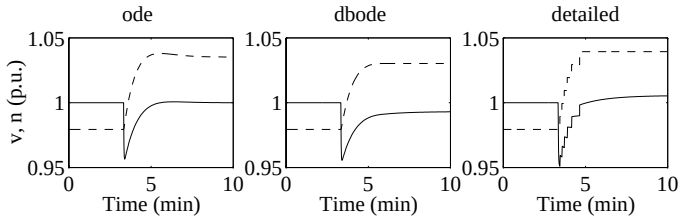

Figure 6.2 Response to voltage disturbance for the three OLTC models - Load side voltage (solid line) and tap ratio (dashed line).

6.3 Small Signal Stability Analysis

The system equilibrium can be found by solving the equations $f(x, V) = g(x, V, n) = 0$ for the unknowns x, n and δ. Linearising (6.1)-(6.2) around the equilibrium point yields

$$\frac{d(\Delta x)}{dt} = \frac{\partial f}{\partial x}\Delta x + \frac{\partial f}{\partial V}\Delta V \tag{6.7}$$

$$0 = \frac{\partial g}{\partial x}\Delta x + \frac{\partial g}{\partial V}\Delta V + \frac{\partial g}{\partial n}\Delta n \tag{6.8}$$

Eliminating ΔV from (6.7), the linearised system model can be written in the standard state space form with Δn as an input and ΔV as an output. That is,

$$\frac{d(\Delta x)}{dt} = A\Delta x + B\Delta n \tag{6.9}$$

$$\Delta V = C\Delta x + D\Delta n \tag{6.10}$$

where $A = \frac{\partial f}{\partial x} - \frac{\partial f}{\partial V}(\frac{\partial g}{\partial V})^{-1}\frac{\partial g}{\partial x}$, $B = -\frac{\partial f}{\partial V}(\frac{\partial g}{\partial V})^{-1}\frac{\partial g}{\partial n}$, $C = -(\frac{\partial g}{\partial V})^{-1}\frac{\partial g}{\partial x}$ and $D = -(\frac{\partial g}{\partial V})^{-1}\frac{\partial g}{\partial n}$. The state space form has the more convenient transfer function equivalent

$$G_n(s) = C(sI - A)^{-1}B + D \tag{6.11}$$

By combining the *ODE* OLTC model with the linearised system model, small signal stability analysis is made using the parameter values given in Table 6.2. Figure 6.3 shows a contour map of the real part of the dominant mode eigenvalue as a function of the OLTC time delay (T) and the load scale factor (k). The stability bound is thus given by the 0-contour. Two observations that can be made regarding the system small disturbance stability are

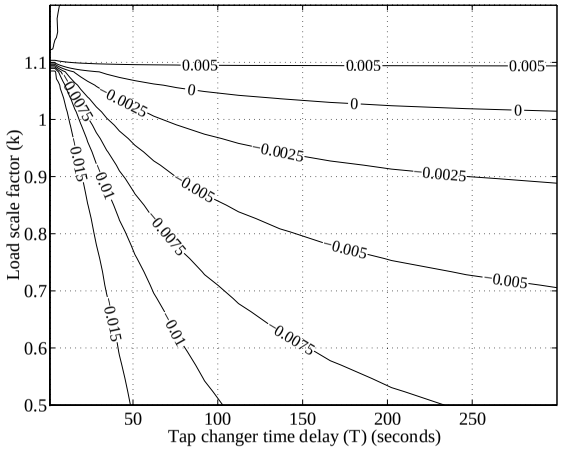

Figure 6.3 Stability contours as a function of load factor (k) and OLTC time delay (T).

as follows: first, for $T = 30$ s, the system is stable if $k < 1.082$, and second, for $k < 0.986$, the system is stable for all positive T. In the next sections, these stability results will be verified by simulation.

6.4 Mechanisms in the Limit Cycle Phenomenon

To illustrate the contributing mechanisms to the limit cycle phenomenon, a simulation is made using the *Detailed* OLTC model. The reactive load has been made over-compensated by setting $B_0 = 0.6$ p.u. The other parameter values are as given in Table 6.2 and the load factor is set to $k = 1$.

Referring to the simulation results in Figure 6.4, the course of events is as follows. Initially, the voltage deviation is positive and growing. When the dead-band is exceeded, the timer is started. As soon as the timer expires, a tap operation is made and the new operating point is determined by the change in tap ratio, the change in reactive output from the capacitor bank and the instantaneous load relief according to $P_t(V)$. As the load recovers to the value dictated by $P_s(V)$, the load side voltage decreases further, and consequently decreases capacitor bank output too. If the capacitor bank and load recovery are sufficiently strong, as is the case here, the voltage continues to decrease until a reverse tap operation is executed.

Voltage then starts increasing due to the change in tap ratio, capacitor

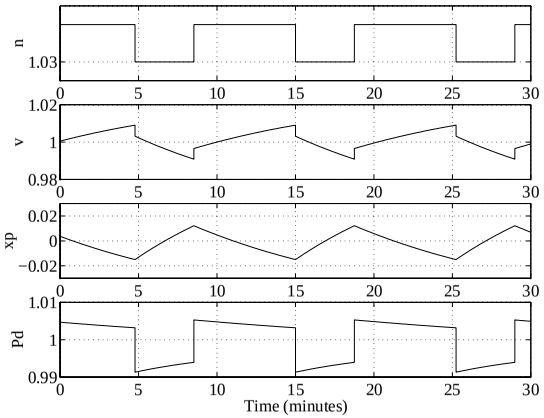

Figure 6.4 Limit Cycle.

bank output and load response. The influence of the load dynamics is now opposite compared to the downward tap operation and voltage now increases until a new downward tap operation is necessary. The resulting cyclic behaviour is called a *limit cycle*.

From this simulation it is evident that a limit cycle results from an interaction between OLTC dead-bands, OLTC and load dynamics accompanied by the load/capacitor voltage sensitivity.

Note however that the instability observed in this example originates from the unstable load dynamics (including capacitor bank) and the interaction between load and tap changer. This indicates that it is not possible to avoid limit cycle behaviour just by re-tuning the OLTC dead-bands or time delays. This issue will be further discussed in Section 6.5 where an analytical insight is given using the describing function method and time simulation.

6.5 Describing Function Analysis

The describing function method can be used to predict existence, period time and amplitude of limit cycles in linear systems under nonlinear feedback such as shown in Figure 6.5b. A thorough presentation of the describing function method along with describing functions of some standard nonlinearities are given in [Hsu and Meyer, 1968].

The method is based on the assumption that since all limit cycles are

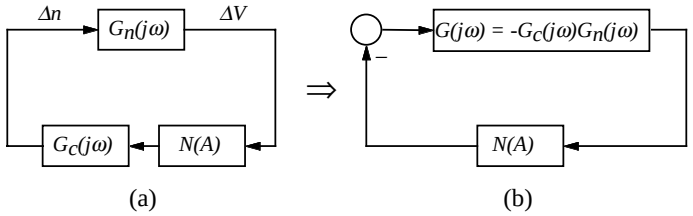

Figure 6.5 Schematic of the feedback loop used in the describing function analysis.

periodic, they are approximately sinusoidal. This assumption is reasonable if the transfer function $G(s)$ in Figure 6.5b has low pass characteristics, i.e., filters out higher order harmonics. The linearised model $G_n(s)$ given by (6.11) does not have this property (since the matrix D in (6.10) is nonzero). However when lumped with the ODE part of the *DBODE* model denoted by $G_c(s)$ in Figure 6.5a, it achieves this.

The describing function of the dead-band in the *DBODE* model is [Hsu and Meyer, 1968]

$$N(A) = \begin{cases} 1 - \frac{2}{\pi}\left(\sin^{-1}(\frac{DB}{2A}) + \frac{DB}{2A}\sqrt{1-(\frac{DB}{2A})^2}\quad\right) \\ \text{if } A > DB/2 \\ 0 \text{ if } A < DB/2 \end{cases} \tag{6.12}$$

where A is the amplitude of a sinusoidal input. A necessary condition for existence of a limit cycle is [Hsu and Meyer, 1968]

$$G(j\omega) = -\frac{1}{N(A)} \tag{6.13}$$

This equation is not easily solved analytically in terms of load and OLTC model parameters, but can be solved graphically or numerically. A limit cycle exists for each intersection of the curves $G(j\omega)$ and $-1/N(A)$ in a Nichols diagram. From the point of intersection the amplitude and frequency of the limit cycle are approximately determined.

In Figure 6.6 the two curves are shown for different values of k in the interval [0.8, 1.1] and $T = 30$ s. The following three cases can be distinguished:

1. $k < 0.986$, the open loop system $G(s)$ has only stable poles, the closed loop system is stable, the phase changes from $-90°$ at low frequencies to $-90°$ at high frequencies, no intersection can occur (dotted lines);

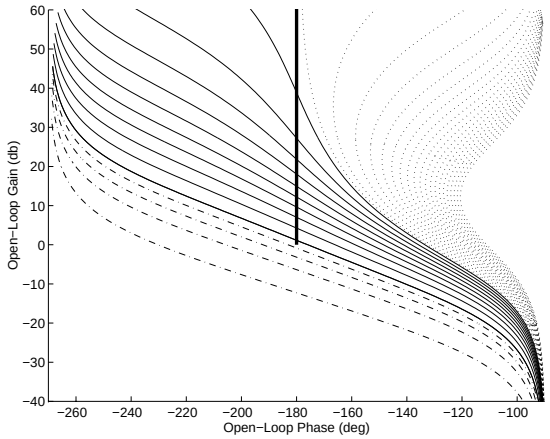

Figure 6.6 Nichols diagram of $G(j\omega)$ for different values of k in the interval [0.8, 1.1] ($T = 30$ s). The thick line is $-1/N(A)$.

2. $0.987 < k < 1.082$, the open loop system has one unstable pole, the closed loop system is stable, the phase changes from $-270°$ at low frequencies frequencies to $-90°$ at high frequencies, one intersection (thin solid lines);

3. $k > 1.083$, the open loop system has one unstable pole, the phase changes from $-270°$ at low frequencies to $-90°$ at high frequencies, the closed loop system experiences instability, no intersection (dash-dotted lines).

In case 2, the intersection indicates that a limit cycle exists. The amplitude of the limit cycle is determined by the curve $-1/N(A)$ which depends only on the dead-band size and the frequency is determined from the curve $G(j\omega)$ that is independent of the dead-band size. The describing function always maps on a line between $(0\text{dB}, -180°)$ and $(\infty, -180°)$ regardless of the dead-band size. It implies that a change in the dead-band size does not affect the existence of a limit cycle. The change in time constants, such as time delay or load recovery time constants, affects $G_c(j\omega)$ as a gain factor and therefore shifts the curve $G(j\omega)$ up or down in the Nichols plot. Consequently the amplitude can be changed, but not the frequency. Shifting the curve below the point $(0\text{dB}, -180°)$ could remove a limit cycle, but would also cause instability of the closed loop system. Note however that load scaling (k) and the voltage sensitivity parameters of the load have a significant

influence, and can affect existence, frequency and amplitude of limit cycles, since they directly affect the shape and position of the curve $G(j\omega)$.

Simulation is used to verify the predictions of the existence and stability of limit cycles. Figure 6.9 (top) illustrates the stable system behaviour for the lower bound on k ($k = 0.986$) along with the describing function analysis result which correctly predicts that the system is free from limit cycles. Increasing the value of k yields to limit cycles of various amplitudes. *Alim* and *Tlim* given in the figure denote the amplitude and period time of limit cycle as predicted by the describing function method. As can be seen from Figure 6.9, the limit cycle amplitude is predicted accurately for all values of k, but the frequency is not for small k. For $k = 1.09$, no limit cycle is present, but the closed loop system is unstable as predicted by the small-disturbance and describing function analysis. Note that for the describing function method to provide an accurate prediction of the limit cycle frequency, the two curves $G(j\omega)$ and $-1/N(A)$ should intersect at an angle as close as possible to 90°. Referring to Figure 6.9, it is clear that for the smaller values of k, the angle of intersection deviates increasingly from the ideal 90°. The logarithmic scale of the y-axis partly conceals this deviation in Figure 6.9.

6.6 Comparison of OLTC Models

In this section the sensitivity of system behaviour to OLTC modelling is investigated for a highly loaded power system. Figure 6.7 presents simulation results obtained with $k = 1$ and $T = 30$ s. As seen in the figure, the system exhibits stable behaviour with the *ODE* model. This is in agreement with small-disturbance stability analysis. For the models that contain the dead-band though, there are limit cycles with an amplitude of 0.01 p.u. and different frequencies, depending on the OLTC model used.

The small disturbance analysis in Section 6.3 also indicates, that the system with the *ODE* model is unstable if the load dynamics is sufficiently fast compared to the OLTC time delay. This is illustrated in Figure 6.8 (top left) for $k = 1$, $T = 120$ s and $T_p = T_q = 10$ s. The system remains unstable with the *DBODE* model too, but the extra lag introduced by the dead-band causes the oscillations to grow more rapidly and voltage collapse occurs one period earlier for that model than for the *ODE* model. However with the *Detailed* model the system exhibits a limit cycle preventing the occurrence of oscillatory voltage instability.

From the simulations in this section, we see that the modelling of the OLTC has a significant effect on the behaviour of the system model.

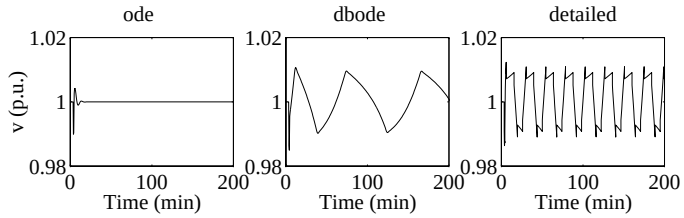

Figure 6.7 Simulations of feeding voltage disturbance for different OLTC models. $k = 1$, $T = 30$ s.

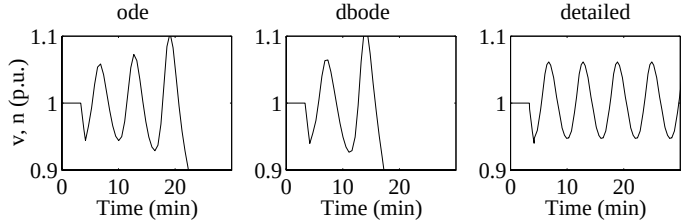

Figure 6.8 Simulations of feeding voltage disturbance for different OLTC models. $k = 1$, $T = 120$ s, $T_p = 10$ s, $T_q = 10$ s.

6.7 Discussion

The describing function analysis results in terms of conditions for limit cycle existence, presented in Section 6.5, are valid only for the *DBODE* OLTC model. Nevertheless, the analysis has clearly shown that the limit cycle phenomena are related to the load dynamics, dead-bands and the interaction between load and tap changer. It has also been shown that the limit cycles are present in the mathematical model of the power system and not due to numerical problems in the simulation. A similar analysis for the *Detailed* OLTC model is possible but would require a derivation of the describing functions corresponding to the nonlinearities present in that model. Note that, since those nonlinearities have memory, the describing functions will be frequency dependent as well as amplitude dependent.

Because of the well-known limitations of the describing function method [Hsu and Meyer, 1968], only a single load single OLTC system has been considered here. However, the simulation of a power system model with cascaded OLTCs has been shown to exhibit a similar or even greater tendency to self-oscillate [Hiskens and Hill, 1993, Popović et al., 1996a].

A somewhat surprising conclusion that can be made is that the limit cycles cannot necessarily be avoided by adjusting the OLTC dead-band or time delay. The explanation is that when the voltage deviation is within the dead-band, the system effectively operates in open loop. As soon as the dead-band is exceeded, the control loop is closed again and the instability is arrested. Referring to Figure 6.6, a necessary condition for the limit cycle to appear is that the open loop system is unstable (due to capacitor bank and load dynamics interaction). If that is the case, an increase of the dead-band size will only increase the amplitude of a limit cycle but will not remove it. Similarly, the different time delays in the OLTC control system have no influence on the existence of limit cycles, only on the amplitude and period time. The only parameters which can affect the existence of limit cycles are load and network parameters. Note that for the sake of getting more insights into the role of dead-bands and load-tap interaction in creating the cyclic behaviour, the tap limits were turned off in our study. That potential source of limit cycles is illustrated in [Vournas and Cutsem, 1995].

Despite the lack of clear evidence for the dead-band and load-tap interaction related limit cycles occurring in power systems, the analysis presented here offers an analytical study which clearly illustrates the potential for this sort of phenomena arising in nonlinear highly stressed power systems.

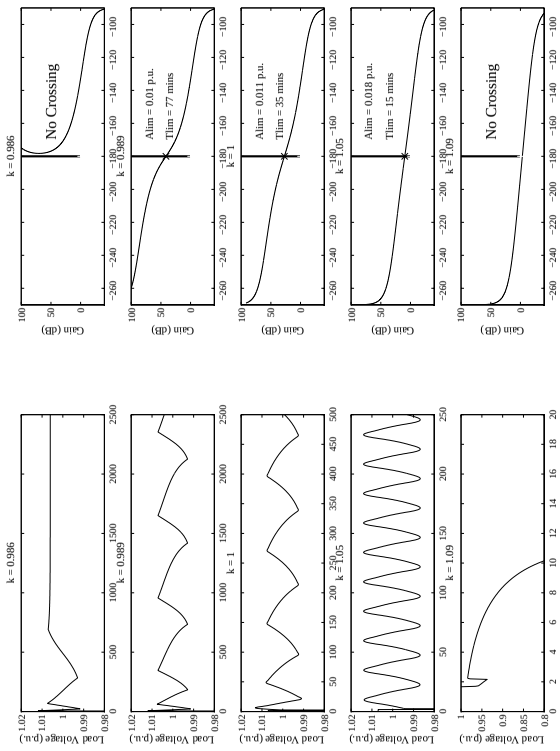

Figure 6.9 Simulations and describing function analysis with different k, ($T = 30$ s, $DBODE$ model).

7

Future Work

There is no pleasure in having nothing to do; the fun is having lots to do and not doing it.

John W. Raper

7.1 Emergency Control of Tap Changers

A variety of sources of voltage instability and collapse have been observed. Occasionally, these incidents are caused by rapid load increase but more often by faults in the transmission system or tripping of generating units. Regardless of the cause, relieving the transmission system of sufficient amount of load in the weak buses will make the system return to a stable condition. Similarly, increasing the load at the weak buses will aggravate the stability problem.

Today, the conventional OLTC controllers aim to restore the load-side voltages and thereby the load power following a voltage drop in the feeding system. With the introduction of centralised distribution network voltage control, it will be possible to use alternative control strategies for the distribution OLTCs during instability incidents. The coordinated controllers presented in this thesis already ensure that unnecessary voltage and thereby load overshoot is avoided in case of large voltage disturbances. With coordinated voltage control, load side voltages can be reduced to provide load relief. The field measurements in [Karlsson, 1992] showed that at least a 5 % load relief for a couple of minutes can be achieved by a 5 % voltage reduction. Also, these measurements showed that most loads do not recover fully, but exhibit steady-state voltage dependency so that some of the load relief will be lasting. In addition to the direct load relief due to the load voltage sensitivity, an indirect load relief on the transmission system due to reduced losses

will be present. Although temporary, due to the load recovery dynamics, this load relief may provide valuable time to execute other emergency actions.

An interesting topic for future research is to investigate how the loading on the transmission network depends on the voltage set-points on the lower levels of the distribution systems, and to investigate the impact of distribution network voltage set-points on transmission system voltage stability. The work could possibly be divided in these parts:

- on-line estimation of load parameters, starting point in [Dovan et al., 1987]
- modelling distribution systems as seen from the transmission level [Lind and Karlsson, 1996].
- detection of stability problem in the transmission system [Löf, 1995]
- identification of weak transmission system buses [Arnborg, 1997]
- calculate impact of restored load-side voltages
- determine alternative control strategy for distribution OLTCs, if voltage restoration will aggravate stability problem

The references given here point to relevant results that may be useful, but has to be adapted for this project. The two last points are new research areas and will be the main theme of the continued research.

7.2 Full-Scale Implementation in the Österlen System

During the work resulting in this thesis, the controller was implemented in a single branch of the distribution system at Österlen. Considering a full distribution system will give some additional freedom, since only the customer side voltages have to be accurately regulated. Certain MV voltages can be allowed to fluctuate more, thereby offering possible additional savings in terms of number of tap operations. A full-scale implementation of the rule-based controller in the Österlen system which has 16 substations with OLTCs, is planned for the autumn of 1997.

7.3 Limit Cycles due to OLTC Dead-bands

In Chapter 6, a limit cycle phenomenon arising from load-tap interaction and OLTC dead-bands was investigated. Conditions for the phenomenon to appear were derived for a simple system using an OLTC model accounting

for the OLTC dead-band. It is possible to derive describing functions for the various more accurate OLTC models that have been presented. This would give insights into the conditions for which the phenomenon will appear using these models. Work in this direction is already in progress and will be submitted for publication shortly.

8

Conclusions

Hofstadter's Law:

It always takes longer than you expect, even when you take Hofstadter's Law into account

In Chapters 2-5 the problem of OLTC control system interaction has been described and three means of improved control have been proposed, each with its own merits:

- new tuning of conventional controllers
- a centralised controller operating on the basis of on-line tap optimisation
- a centralised controller operating on the basis of fuzzy-set manipulation

The first solution obviously has the merit that the existing controllers are preserved, so that no new investments are necessary. Therefore this is suitable as a first step, before a centralised controller is implemented. The simulation results in Chapter 5 indicate that about a 10 % reduction of the number of tap operations is achieved in the three-OLTC test system.

The two new controllers rely on communication between sub-stations. The simulation results indicate a reduction of the total number of operations by about 36 % compared to conventional scheme with the new tuning, with the fuzzy-rule based controller. The additional reduction with the optimal controller is about 45 % compared to the conventional controllers and 14 % compared to the rule-based controller. The optimal controller relies also on a network model and is suitable for implementation as part of a DA system that can provide an up-to-date network model, whereas the fuzzy rule-based controller can be implemented on its own. The optimal controller was also used as a benchmark during the design of the rule-based controller. The

fuzzy-rule based controller was used in a prototype that has been tested in the rural distribution system at Österlen.

In Chapter 6 the phenomenon of limit cycle behaviour due to tap changer dead-bands and load-tap interaction has been investigated. Also, the effect of tap dynamics modelling on system behaviour has been illustrated. It has been shown that the results from small disturbance analysis based on a continuous OLTC model are unreliable, especially in a heavily loaded power system. Under heavy load conditions, the system with a detailed OLTC model exhibits a limit cycle that will arrest oscillatory voltage instability predicted by small disturbance analysis. The key parameters in creating/avoiding this kind of limit cycles are identified as the system load level, degree of reactive compensation and the load voltage dependency. In certain loading conditions, adjusting OLTC control system parameters such as time delays or dead-band size is shown not to have any effect on the existence of the limit cycles.

A

System Models

For those who like this sort of thing, this is the sort of thing they like.

Abraham Lincoln

A.1 Test system A.1

In this appendix, the mathematical modelling and parameter data for the Österlen test system in Figure 2.10 is given. Combining the individual component models given in section 2.1 with power balance equations, a model of the system can be written in the differential-algebraic form

$$\dot{x} = f(x, V) \tag{A.1}$$
$$0 = g(x, V, u) \tag{A.2}$$

where

$$x = [x_{p2}\ x_{q2}\ x_{p3}\ x_{q3}\ x_{p4}\ x_{q4}]^T \tag{A.3}$$
$$V = [v_1\ v_2\ v_3\ v_4\ \delta_1\ \delta_2\ \delta_3\ \delta_4]^T \tag{A.4}$$
$$u = [n_1\ n_2\ n_3\ B]^T. \tag{A.5}$$

x is the dynamic state vector and V is the algebraic state vector. The transformer tap ratios (n_i) and the capacitor bank susceptance (B) are considered to be controllable variables (u). Functions f and g are then defined by equations (A.6)-(A.7).

During the work resulting in [Lind and Karlsson, 1996], a model of the complete distribution system at Österlen was derived along with reduced

Load Data					
α_s	α_t	T_p	β_s	β_t	T_q
1.28	1.92	173	1.32	2.92	83.5

OLTC Data					
TLA					
min tap	*max tap*	*tap step*	$u_{function}$	u_{reset}	T_d
1	19	1.67%	1.50%	1.35%	120 s
JSD					
min tap	*max tap*	*tap step*	$u_{function}$	u_{reset}	T_d
1	9	2.50%	2.25%	2.00%	120 s
ÖTP					
min tap	*max tap*	*tap step*	$u_{function}$	u_{reset}	T_d
1	17	1.67%	1.50%	1.35%	120 s

Network Data							
Z_0 (p.u.)	θ_0 (rad)	Z_1 (p.u.)	θ_1 (rad)	Z_2 (p.u.)	θ_2 (rad)	Z_3 (p.u.)	θ_3 (rad)
0.0561	1.3369	0.0953	1.5584	0.6796	1.3486	2.663	1.4958

p.u. Conversion Data		
Vbase (130 kV level)	*Vbase (50 kV level)*	*Vbase (20 kV level)*
132 kV	*55 kV*	*22kV*
Vbase (10 kV level)	*Sbase*	
10.7 kV	*100 MVA*	

Table A.1 Parameter values for the Österlen test system.

models intended for use in voltage stability studies. The author of this work has supplied the network parameters used in Table A.1.

$$f(x,V) = \begin{bmatrix} \frac{-x_{p2}+P_{02}v_2{}^{\alpha_{s2}}-P_{02}v_2{}^{\alpha_{t2}}}{T_{p2}} \\ \frac{-x_{q2}+Q_{02}v_2{}^{\beta_{s2}}-Q_{02}v_2{}^{\beta_{t2}}}{T_{q2}} \\ \frac{-x_{p3}+P_{03}v_3{}^{\alpha_{s3}}-P_{03}v_3{}^{\alpha_{t3}}}{T_{p3}} \\ \frac{-x_{q3}+Q_{03}v_3{}^{\beta_{s3}}-Q_{03}v_3{}^{\beta_{t3}}}{T_{q3}} \\ \frac{-x_{p4}+P_{04}v_4{}^{\alpha_{s4}}-P_{04}v_4{}^{\alpha_{t4}}}{T_{p4}} \\ \frac{-x_{q4}+Q_{04}v_4{}^{\beta_{s4}}-Q_{04}v_4{}^{\beta_{t4}}}{T_{q4}} \end{bmatrix} \tag{A.6}$$

$$g(x,V,n) = \begin{bmatrix} \frac{v_1{}^2\cos(\theta_0)}{Z_0} - \frac{v_1v_2\cos(\delta_2-\theta_1-\delta_1)}{Z_1n_1} - \frac{Vv_1\cos(\theta_0+\delta_1)}{Z_0} + \frac{v_1{}^2\cos(\theta_1)}{Z_1n_1{}^2} \\ -\frac{Vv_1\sin(\theta_0+\delta_1)}{Z_0} + \frac{v_1{}^2\sin(\theta_0)}{Z_0} + \frac{v_1v_2\sin(\delta_2-\theta_1-\delta_1)}{Z_1n_1} - v_1{}^2B + \frac{v_1{}^2\sin(\theta_1)}{Z_1n_1{}^2} \\ -\frac{v_2v_3\cos(-\delta_3+\theta_2+\delta_2)}{Z_2n_2} - \frac{v_1v_2\cos(\delta_2+\theta_1-\delta_1)}{Z_1n_1} + \frac{v_2{}^2\cos(\theta_2)}{Z_2n_2{}^2} + \frac{v_2{}^2\cos(\theta_1)}{Z_1} + x_{p2} + P_{02}v_2{}^{\alpha_{t2}} \\ \frac{v_2{}^2\sin(\theta_1)}{Z_1} - \frac{v_2v_3\sin(-\delta_3+\theta_2+\delta_2)}{Z_2n_2} + \frac{v_2{}^2\sin(\theta_2)}{Z_2n_2{}^2} - \frac{v_1v_2\sin(\delta_2+\theta_1-\delta_1)}{Z_1n_1} + x_{q2} + Q_{02}v_2{}^{\beta_{t2}} \\ -\frac{v_2v_3\cos(-\delta_3-\theta_2+\delta_2)}{Z_2n_2} + \frac{v_3{}^2\cos(\theta_3)}{Z_3n_3{}^2} - \frac{v_3v_4\cos(\delta_4-\theta_3-\delta_3)}{Z_3n_3} + \frac{v_3{}^2\cos(\theta_2)}{Z_2} + xp_3 + P_{03}v_3{}^{\alpha_{t3}} \\ \frac{v_3{}^2\sin(\theta_2)}{Z_2} + \frac{v_2v_3\sin(-\delta_3-\theta_2+\delta_2)}{Z_2n_2} + \frac{v_3v_4\sin(\delta_4-\theta_3-\delta_3)}{Z_3n_3} + \frac{v_3{}^2\sin(\theta_3)}{Z_3n_3{}^2} + xq_3 + Q_{03}v_3{}^{\beta_{t3}} \\ -\frac{v_3v_4\cos(\delta_4+\theta_3-\delta_3)}{Z_3n_3} + \frac{v_4{}^2\cos(\theta_3)}{Z_3} + x_{p4} + P_{04}v_4{}^{\alpha_{t4}} \\ -\frac{v_3v_4\sin(\delta_4+\theta_3-\delta_3)}{Z_3n_3} + \frac{v_4{}^2\sin(\theta_3)}{Z_3} + x_{q4} + Q_{04}v_4{}^{\beta_{t4}} \end{bmatrix} \tag{A.7}$$

A.2 Test system A.2

In this appendix, the mathematical modelling and parameter data for the smaller example system in Figure 2.2 are given.

$$f(x,V) = \begin{bmatrix} \frac{-x_p + P_0 v_2{}^{\alpha_s} - P_0 v_2{}^{\alpha_t}}{T_p} \\ \frac{-x_q + Q_0 v_2{}^{\beta_s} - Q_0 v_2{}^{\beta_t}}{T_q} \end{bmatrix} \tag{A.8}$$

$$g(x,V,n) = \begin{bmatrix} \frac{v_1{}^2 \cos(\theta_0)}{Z_0} - \frac{V v_1 \cos(\theta_0+\delta_1)}{Z_t n} Z_0 - \frac{v_1 v_2 \cos(-\theta_t-\delta_1+\delta_2)}{Z_t n} + \frac{v_1{}^2 \cos(\theta_t)}{Z_t n^2} \\ \frac{v_1{}^2 \sin(\theta_0)}{Z_0} + \frac{v_1{}^2 \sin(\theta_t)}{Z_t n^2} Z_t n^2 - v_1{}^2 B - \frac{v_1 v_2 \sin(\theta_t+\delta_1-\delta_2)}{Z_t n} - \frac{V v_1 \sin(\theta_0+\delta_1)}{Z_0} \\ -\frac{v_1 v_2 \cos(\theta_t-\delta_1+\delta_2)}{Z_t} Z_t n + \frac{v_2{}^2 \cos(\theta_t)}{Z_t} + x_p + P_0 v_2{}^{\alpha_t} \\ -\frac{v_1 v_2 \sin(\theta_t+\delta_1+\delta_2)}{Z_t n} + \frac{v_2{}^2 \sin(\theta_t)}{Z_t} + x_q + Q_0 v_2{}^{\beta_t} \end{bmatrix} \tag{A.9}$$

A.3 Neuron C Definitions for the TapTalk Protocol

```
#ifndef _globaldefs_h
#define _globaldefs_h 1

#include <float.h>

#define flt (const float_type *)

typedef float_type utype;
typedef float_type ptype;
typedef float_type qtype;

typedef signed int   ext_controltype;
typedef signed int   tap_postype;

typedef struct {
                signed long    t1;
                signed long    t2;
              } tap_counttype;

/* stations */
typedef enum { tla, jsd, otp } stationtype;

/* tap changer control modes */
typedef enum{ off, local, rem_abs, rem_rel,
              mod_slave } control_modetype;

/* tap alarms */
typedef enum {ok, tap_upper_limit, tap_lower_limit,
              tap_malfunction, program_error,
              comm_timeout, max_dev_exc } tap_alarmtype;

/* messagetypes */
typedef enum { measurements, controls } messagetypetype;

/* measurement structure */
typedef struct
        {
          control_modetype      controlmode;
          tap_postype           tap_pos;
          tap_alarmtype         tap_alarm;
```

```
        utype           u;
        ptype           p;
        qtype           q;
        utype           uref;
      } measdatatype;

/* controls structure */
typedef enum  {setcontrolmode, setextcontrol, tap_init}
            controltypetype;

typedef union {
              control_modetype    mode;
              ext_controltype     ext_control;
              tap_postype         tap_pos_init;
              utype               uref;
            } ctrltmptype;

typedef union
      {
        controltypetype controltype;
        ctrltmptype data;
      } controldatatype;

typedef struct  {
          measdatatype meas;
          controldatatype control;
        } msgdatatype;


/* message type */
typedef struct msgtype
      {
        stationtype         sender;
        stationtype         receiver;
        messagetypetype     messagetype;
        msgdatatype         data;
      } messagetype;

// typedef struct msgtype *message_ptype;


#endif
```


B

Glossary and Nomenclature

Wethern's Law:

Assumption is the mother of all screw-ups.

B.1 Nomenclature

A_{lim}	predicted amplitude of limit cycle
A, B, C, D	matrices defining standard state-space form
B_0	capacitor bank susceptance
c_i	penalty weight for voltage deviation at bus i
d_j	penalty weight for change of tap ration of OLTC j
DB	tap changer dead-band ($DB = 2u_{\text{function}}$)
$f(x, V)$	dynamic state derivative function of DA model.
$F(\mathbf{x})$	objective function used in optimal control scheme
$g(x, V, n)$	algebraic equations of DA model.
$G(\mathbf{x})$	equality constraints in optimal control scheme
$G(s)$	transfer function
$H(\mathbf{x})$	inequality constraints in the optimal controller
k	load scaling parameter, enumeration variable
n	tap ratio
$N(A)$	describing function

P_{ij}	active power transported from node i to j
P_0	connected active load
P_d	actual active power load demand
$P_s(V)$	active power steady-state voltage dependency
$P_t(V)$	active power transient voltage dependency
Q_{ij}	reactive power transported from node i to j
Q_0	connected reactive load
Q_d	actual reactive power load demand
$Q_s(V)$	reactive power steady-state voltage dependency
$Q_t(V)$	reactive power transient voltage dependency
T_{lim}	predicted period time of limit cycle
T_p	active power load recovery time constant
T_q	reactive power load recovery time constant
T_{d0}	tap changer delay time (tuning parameter)
T_d	tap changer delay time (actual)
T_m	mechanical delay time of tap changer
T_{count}	tap changer timer value
UP_{TLA}	fuzzy set describing to what degree an upward tap operation should be made the station TLA.
$DOWN_{TLA}$	fuzzy set describing to what degree a downward tap operation should be made the station TLA.
u_{function}	tap changer function voltage
u_{reset}	tap changer reset voltage
V	infinite bus voltage, algebraic state vector in DA model
V_N	nominal voltage
v_{dev_i}	voltage deviation at bus i
$v_i \angle \delta_i$	complex voltage at bus i
v_r	voltage reference value

$\mathbf{x}$	vector of tap positions, used as optimisation variable in optimal control scheme
x	load state vector in DA model
x_p	dynamic active power load state
x_q	dynamic reactive power load state
$\mathbf{x}$	vector of tap positions and auxiliary variables in the optimal control scheme
X	reactance in p.u.
$Z_i \angle \theta_i$	complex impedance of line or transformer i
α_s	active power steady-state voltage dependency exponent
α_t	active power transient voltage dependency exponent
β_s	reactive power steady-state voltage dependency exponent
β_t	reactive power transient voltage dependency exponent
$\wedge$	fuzzy set intersection operator (AND)
$\vee$	fuzzy set union operator (OR)
$\neg$	fuzzy set complement operator (NOT)

B.2 Glossary

CCN	Conventional Controllers with Normal Tuning
CCR	Conventional Controllers with Revised Tuning
CIGRE	Conférence Internationale des Grands Réseaux Electriques
Control Surface	Diagram showing the mapping between two measurements and one control signal.
CRC	Cyclic Redundancy Checksum
DA	Distribution Automation.

DBODE Ordinary differential equation model of an OLTC which has been augmented with a deadband at the voltage input

DDE Dynamic Data Exchange

Defuzzification The process of translating a fuzzy variable to physical quantity.

Detailed Detailed model of an OLTC according to Section 3.2

EdF Electricité de France

EPRI Electrical Power Research Institute

FRB Fuzzy Rule Based Controller

Fuzzification The process of making a fuzzy set interpratation of a physical measurement.

HA Home Automation.

HV network High Voltage network ($80 \leq V_N < 220$ kV), in Sweden typically 130 kV subtransmission network.

IEC International Electrotechnical Comission

IEEE Institute of Electrical and Electronics Engineers

Inference The process of mapping measurements to control actions in a fuzzy controller.

JSD Jãrrestad

Load Curve Curve showing the daily load variations.

LV network Low Voltage network (0.4 kV)

MV network Medium Voltage network ($10 \leq V_N < 80$ kV), in Sweden typically 220 or 400 kV transmission network.

Network Variable Special variable used for communication between LonWorks nodes.

ODE Ordinary differential equation model of an OLTC

OLTC On Load Tap Changer, device capable of changing the number of active windings on a transformer while it is in operation. Same as LTC (Load Tap Changer), ULTC (Under Load Tap Changer) and TCUL (Tap Changer Under Load).

OPT Optimal Controller

Optimal Power Flow (OPF) The problem of determining optimal voltage setpoints for generators, tap positons and capacitor bank status to achieve as small losses as possible in a transmission system.

OSI Open Systems Interconnection, standard for communication protocol structuring

OTP Östra Tommarp

RS-232 Standard for serial communication, for example from a PC to a modem

Rule-Base A set of linguistic rules describing the mapping measurements to control actions in a fuzzy controller.

SCADA System Supervisory Control And Data Acquisition System. Automation equipment for control an monitoring of the transmission system.

Selectivity The ability of an OLTC control scheme to perform tap operations in correct sequence.

TLA Tomelilla

TP Twisted pair, 78 kbps bus network.

Unit Commitment (UC) The problem of optimal scheduling of generators to achieve minimum generation cost.

VHV network Very High Voltage network ($V_N \geq 220$ kV) - typically 220 or 400 kV transmission network in Sweden.

Voltage Step Voltage change of 1 % or more in less than 1 second

C

References

Westheimer's Discovery:

A couple of months in the laboratory can frequently save a couple of hours in the library.

[Abe et al., 1982] Abe, S., Fukunaga, Y., Isono, A., and Kondo, B. (1982). Power system voltage stability. *IEEE Transactions on Power Apparatus and Systems*, PAS-101(10):3830–3840.

[Altsjö, 1993] Altsjö, K. (1993). Modellering av spänningsregulator för lindningskopplare. Master's thesis, Electrical and Computer Engineering, Chalmers Institute of Technology, Sweden. Examensarbete 92/93:02 (in Swedish).

[Arnborg, 1997] Arnborg, S. (1997). *Emergency Control of Power Systems in Voltage Unstable Conditions*. PhD thesis, Dept. of Electric Power Engineering, Royal Institute of Technology, Sweden. TRITA-EES-9701.

[Ćalović, 1984] Ćalović, M. S. (1984). Modelling and analysis of under-load tap-changing transformer control system. *IEEE Transactions on Power Apparatus and Systems*, PAS-103(7):1909–1915.

[Carbone et al., 1996] Carbone, F., Castellano, G., and Moreschini, G. (1996). Coordination and control of tap changers under load at different voltage level transformers. In *Proceedings of Melecon '96, Rome*.

[Dovan et al., 1987] Dovan, T., Dillon, T. S., Berger, C. S., and Forward, K. A. (1987). A microcomputer based on-line identification approach to power system dynamic load modelling. *IEEE Transactions on Power Systems*, 2(3):529–535.

[Ericsson, 1997] Ericsson, L. (1997). *Dynamic Load Control - Power Peak Shaving applied to a Foundry*. Licenciate thesis, Dept. of Industrial Electrical Engineering and Automation, Lund Institute of Technology, ISBN 91-88934-06-3.

[Hiskens and Hill, 1993] Hiskens, I. A. and Hill, D. J. (1993). Dynamic interaction between tapping transformers. In *Proceedings of 11th Power Systems Computation Conference*. Avignon, France.

[Hsu and Meyer, 1968] Hsu, J. C. and Meyer, A. U. (1968). *Modern Control Principles and Applications*. Mc-Graw Hill.

[IEEELoad, 1995] IEEELoad (1995). Standard load models for power flow and dynamic performance simulation. *IEEE Transactions on Power Systems*, 10(3):1302–1313.

[IEEESVC, 1994] IEEESVC (1994). Static var compensator models for power flow and dynamic performance simulation. *IEEE Transactions on Power Systems*, 9(1):229–240.

[Jantzen, 1991] Jantzen, J. (1991). *Fuzzy Control*. Technical University of Denmark. Publ. no. 9109.

[Karlsson, 1992] Karlsson, D. (1992). *Voltage Stability Simulations using Detailed Models Based on Field Measurements*. PhD thesis, Electrical and Computer Engineering, Chalmers Institute of Technology, Göteborg, Sweden. Tech. Report no. 230.

[Karlsson, 1993] Karlsson, D. (1993). Kaskadkopplade lindningskopplare, inledande registreringar. Internal Report PTS-9309-62, SYDKRAFT AB, Malmö, Sweden (in Swedish).

[Karlsson and Hill, 1994] Karlsson, D. and Hill, D. J. (1994). Modelling and identification of nonlinear dynamic loads in power systems. *IEEE Transactions on Power Systems*, 9(1):157–163.

[Lakervi and Holmes, 1989] Lakervi, E. and Holmes, E. J. (1989). *Electricity distribution network design*. Peregrinus Books. pp. 253-255.

[Larsson and Karlsson, 1995] Larsson, M. and Karlsson, D. (1995). Coordinated control of cascaded tap changers in a radial distribution network. In *Proceedings of IEEE/KTH Stockholm PowerTech Conference, June 18-22*. Publication SPT PS 22-06-0405.

[Lee et al., 1995] Lee, K. Y., Bai, X., and Park, Y. M. (1995). Optimization method for reactive power planning by using a modified simple genetic algorithm. *IEEE Transactions on Power Systems*, 10(4).

[Lee-Smith, 1996] Lee-Smith, H. (1996). Substation automation - problems and possibilities. *Computer Applications in Power*, 9(4).

[Lerch et al., 1992] Lerch, E., Povh, D., and Xu, L. (1992). Advanced svc control for damping power system oscillations. *IEEE Transactions on Power Systems*, 6(2).

[Lind and Karlsson, 1996] Lind, R. and Karlsson, D. (1996). Distribution system modelling for voltage stability studies. *IEEE Transactions on Power Systems*, 11(4).

[Liu and Vu, 1989] Liu, C. C. and Vu, K. T. (1989). Analysis of tap-changer dynamics and construction of voltage stability regions. *IEEE Transactions on Circuits and Systems*, 36(4):575–590.

[Löf, 1995] Löf, P. A. (1995). *On Static Analysis of Long-Term Voltage Stability*. PhD thesis, Dept. of Electric Power Engineering, Electric Power Systems, Royal Institute of Technology, Stockholm, Sweden. TRITE-EES-9501, ISSN 1100-1607.

[LRG, 1992] LRG (1992). *Neuron C Programmers Guide*. Echelon Corporation, 4015 Miranda Avenue, Palo Alto, California, 94304.

[Medanić et al., 1987] Medanić, J., Ilić-Spong, M., and Christensen, J. (1987). Discrete models of slow voltage dynamics for under load tap-changing transformer coordination. *IEEE Transactions on Power Systems*, 2(4):873–882.

[Nara et al., 1992] Nara, K., Shiose, A., Kitagawa, M., and Ishihara, T. (1992). Implementation of genetic algorithm for distribution systems loss minimum reconfiguration. *IEEE Transactions on Power Systems*, 7:1044–1050.

[Partanen et al., 1994] Partanen, J., Järventausta, P., Verho, P., and Kärenlampi, M. (1994). A support system for fault location and restoration of mv-feeders. In *Nordic Distribution Automation Conference*.

[Popović, 1995] Popović, D. H. (1995). *Modelling, Stability and Control of Voltage Behaviour in Power Supply Systems*. PhD thesis, Dept. of Electrical and Computer Engineering, University of Newcastle.

[Popović et al., 1996a] Popović, D. H., Hill, D. J., and Hiskens, I. A. (1996a). Oscillatory behaviour of power supply systems with single dynamic load. In *Proceedings 12th Power Systems Computation Conference*.

[Popović et al., 1996b] Popović, D. H., Hiskens, I. A., and Hill, D. J. (1996b). Investigations of load-tap changer interaction. *International Journal of Electrical Power and Energy Systems*, 18(2):81–97.

[Roytelman et al., 1995] Roytelman, I., Wee, B. K., and Lugtu, R. L. (1995). Volt/var control algorithm for modern distribution management system. *IEEE Transactions on Power Systems*, 10(3).

[Sauer and Pai, 1994] Sauer, P. W. and Pai, M. A. (1994). A comparison of discrete vs. continuous dynamic models of tap-changing-under-load transformers. In *Proceedings of NSF/ECC Workshop on Bulk power System Voltage Phenomena - III : Voltage Stability, Security and Control*. Davos, Switzerland.

[SS 421 18 11, 1989] SS 421 18 11 (1989). Spänningsgodhet i lågspänningsnät för allmän distribution. Technical report, Svenska Elektriska Komissionen. (in Swedish).

[Stallings, 1991] Stallings, W. (1991). *Data and Computer Communications*. Maxwell Macmillan International Editions.

[Vournas and Cutsem, 1995] Vournas, C. D. and Cutsem, T. V. (1995). Voltage oscillations with cascaded load restoration. In *Proceedings of IEEE/KTH Stockholm PowerTech Conference*. Publication SPT PS 22-04-0426.

[Vu and Liu, 1992] Vu, K. T. and Liu, C. C. (1992). Shrinking stability regions and voltage collapse in power systems. *IEEE Transactions on Circuits and Systems-I: Fundamental Theory and Applications*, 39(4):271–289.

[Walve, 1986] Walve, K. (1986). Modelling of power system components at severe disturbances. In *CIGRÉ, Paper 38-18*.

[Wood et al., 1988] Wood, P., Bapat, V., and Putkovich, R. P. (1988). Study of improved load-tap-changing for transformers and phase-angle regulators. Technical report, EPRI. EL-6079.

[Yorino et al., 1996] Yorino, N., Danyoshi, M., and Kitagawa, M. (1996). Interaction among multiple controls in tap change under load transformers. In *IEEE/PES Winter Meeting*. Publication 96 WM 310-3 PWRS.